THE MINISTRY OF NATIONAL
INFRASTRUCTURES
GEOLOGICAL SURVEY OF ISRAEL

# Morphometric Analyses for Determining the Age of Escarpments: An Example from the Galilee, Northern Israel

A. Matmon, E. Zilberman, and Y. Enzel

December 1998
ES/38/98

Report GSI/31/98

THE MINISTRY OF NATIONAL
INFRASTRUCTURES
GEOLOGICAL SURVEY OF ISRAEL

# Morphometric Analyses for Determining the Age of Escarpments: An Example from the Galilee, Northern Israel

A. Matmon[1,2], E. Zilberman[1], and Y. Enzel[2]

1. Geological Survey of Israel
2. Hebrew University

Front Cover: The Zurim Escarpment - A view from Biq'at Bet Kerem

December 1998
ES/38/98

Report GSI/31/98

## Acknowledgments

We would like to thank Yael Krith-Man for the many hours she spent digitizing structural maps, Erez Vienrot, and Adi Ben-nun from the Hebrew University GIS division for teaching us some of the GIS techniques, and their assistance in calculating L-index values, J. Hall for providing the D.T.M. data set and Bat-Sheva Cohen and Nehama Shragai, Graphics division of the GSI, for working with us to improve the maps and graphs. Many thanks to Zvi Garfunkel, R. Amit, S. Horowitz, S. Marco, P. Bierman, and S. Wells for helpful discussions and suggestions, Z. Levy for a very constructive and thorough review and X. Wdowinski for reviewing the English. Part of the funding for this research was provided by Dr. Y. Wieler, Atomic Energy Commission.

## Contents

## List of figures and tables:

# Abstract

Dating of tectonic activity in erosional landscapes is problematic because dateable sediments are absent. We use GIS-based morphometric analyses of escarpments bounded by normal faults in the Galilee as a tool to determine their relative ages. Two morphometric parameters are used to discriminate tectonic phases in this extensional region: a) The ratio L between the height of the escarpment and the total stratigraphic displacement, b) The shape of the topographic profile of each escarpment relative to a slope profile of known age (Mt. Tur'an). Systematic changes in L-index values along a fault are indicative of segmentation. By comparing the profile shapes it is possible to determine the relative timing for a change in rates of displacement from slow, continuous and landscape-truncating phase, to a fast topography-forming phase.

In order to put time constrain on the evolution of the fault escarpments in the Galilee they were compared to the well dated fault escarpment of Mt. Tur'an, which is ~300 meters high and has a total displacement of 625 m. The fault displaces 300 m vertically a basalt flow 4.23±0.23 Ma old, an offset which is identical to the height of its escarpment. The L-index value for this escarpment is ~0.5, indicating that the Tur'an fault was active prior to 4.23 Ma but at slow uplift rates that enabled truncation to maintain the gentle slope over which the basalt flowed. Increased tectonic rates following the basalt extrusion led to the formation of the present escarpment. The preservation of the basalt at the top of the escarpment indicates that erosional lowering of the upper surface of the Tur'an block has been minor since its formation.

From the comparison between profiles of fault escarpments in the Galilee and from calculating their L-index we conclude that (a) the topographic profiles of different parts of each individual escarpment have similar shapes; (b) there are systematic variations in profiles along escarpments that fit the segmentation deduced from the L-index values; (c) escarpments more concave or convex than the reference escarpment are older or younger than 4 Ma, respectively, and (d) The Galilee escarpments did not form simultaneously. A few were already major morphotectonic features by the Early to Middle Pliocene and the rest are younger, having formed between 4-2 Ma.

# 1. Introduction

Neogene and Quaternary sediments and volcanic rocks accumulated in the eastern Lower Galilee (Schulman, 1962; Shaliv, 1991), along the coastal plain (Kafri and Ecker, 1964; Issar and Kafri, 1972; Sivan, 1996) and in small volcanic fields in the eastern Upper Galilee. However, most of the mountainous area of the Galilee has been subjected to erosion since the Neogene and, therefore, the youngest exposed rocks in this area are of Eocene age. The absence of upper Tertiary sedimentary rocks implies that over most of the Galilee there are very few young stratigraphic markers and datable geologic features that can help in reconstructing the post Eocene tectonic development of the region. Surface dating using cosmogenic isotopes is possible although in most places the exposure and burial history of the exposed rocks is probably too complex for using this method. In specific sites, as will be mentioned later, basalt units do help in understanding local tectonism. For this reason, the understanding of the temporal and spatial development of most of the main morphotectonic features in the Galilee is limited.

Morphological analysis of large-scale fault escarpments enables us to propose a temporal framework for the tectonic activity of the main tectonic blocks in the Galilee. This analysis is based on the assumption that time is the main factor controlling slope development; climate, lithology, soil cover and vegetation are relatively similar and, therefore, can be considered constant throughout the Galilee.

## 2. Previous Studies

Morphologic features in general, and the evolution of the shape of slopes in particular, have been used as tools to study tectonic activity. Bull and McFadden (1977) and Bull (1977) used geomorphic features to describe the relation between tectonics and geomorphologic processes. Adams (1984) points to the secondary influence of lithology on the development of escarpments in the mountain front of the Southern Alps of New Zealand. Hare and Gardner (1984) analyzed uplifted surfaces and density of fragmentation of uplifted blocks to determine relative timing of tectonic activity in Costa Rica. Mayer (1986) proposed several morphologic indices along mountain fronts and escarpments that can be used as tectonic indicators, while Ke(1986) discussed the use of surficial processes as tools for tectonic investigation. Wells et al. (1988) applied geomorphic analysis to variations in tectonic activity along the subducting Cocos plate boundary using mountain front morphology, riverbed gradients and shapes of ridges. Investigation of a tectonic escarpments bounding the Rio Grande rift in New Mexico by Menges (1988) indicates that lithology plays only secondary role in the development of tectonic slopes.

Only a few studies have examined the relation between tectonics and morphology in the Galilee. Yair (1962) analyzed the morphology of Nahal Dishon (Fig. 1) and found a correlation between the main stages of development of the Dishon valley and the subducting pull-apart Hula Valley (Fig. 1). Nir (1970) distinguished morphologic surfaces in the Galilee and attributed them to the recent uplift of the area; however, he did not date the uplifting stages. Bar and Harash (1983) compared slope morphology of different tectonic escarpments in northern Israel and categorized them into several groups according to their shapes. Ron et al.(1984) distinguished between two main tectonic phases in the Galilee: a pre-Pliocene phase that does not contribute to the present morphology and a post-Pliocene phase that controls the present landscape. They also pointed to the occurrence of hanging valleys (on the Rosh-Haniqra escarpment, for example) as indicators of young displacement. Achmon (1986) described left-lateral offset streams along the Carmel fault, indicating recent left-lateral movement. Kafri (1997) reconstructed cross-Galilee Neogene streams by correlating wide wind gaps and relics of conglomerates.

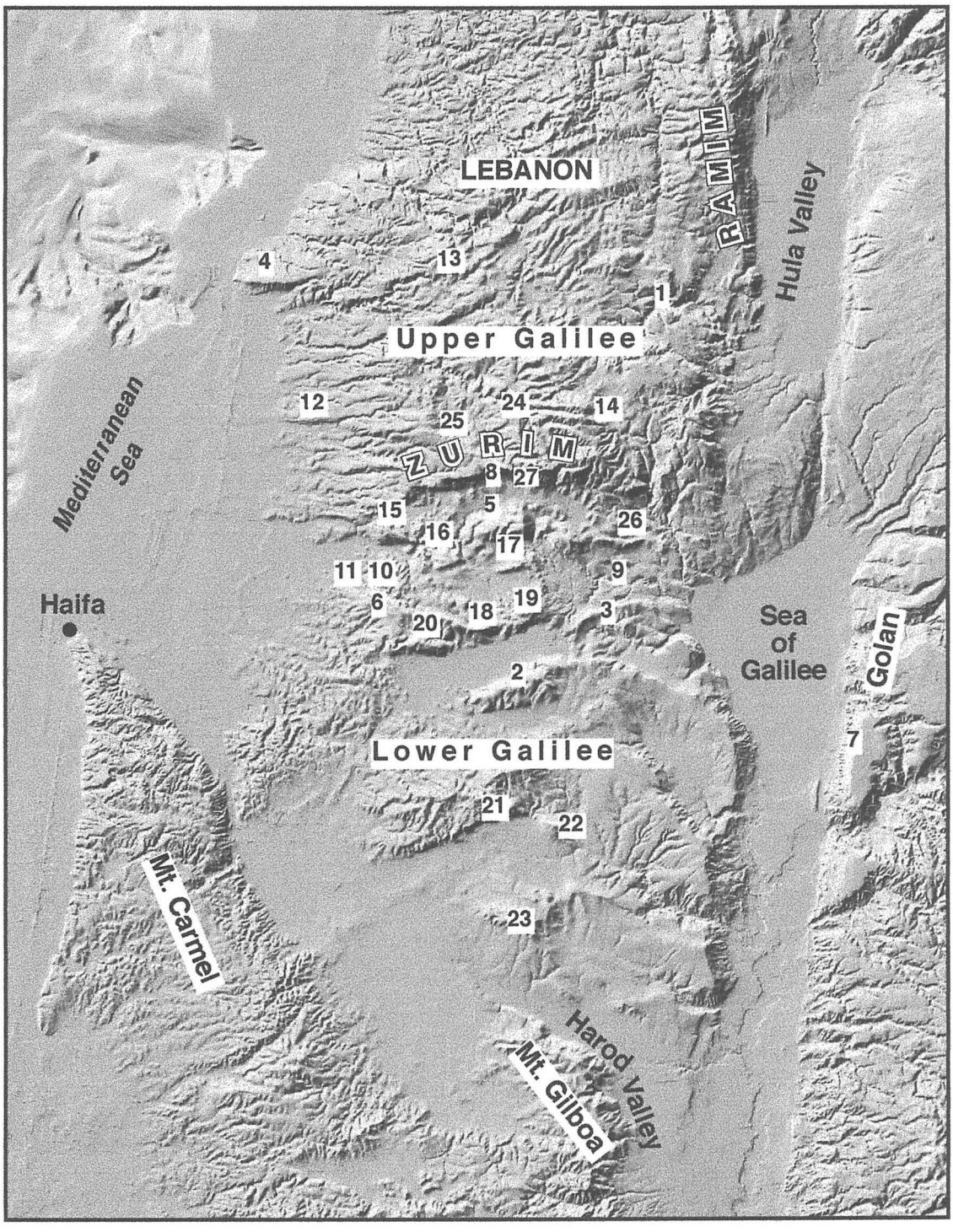


Fig. 1 – Location map.. 1- Nahal Dishon, 2- Mt. Tur'an, 3- Mimlah, 4- Rosh-Haniqra, 5- Kamon, 6- Qoranit, 7- Ha'on, 8- Sahzor, 9- Nahal Zalmon, 10- Nahal Segev, 11- Kabul, 12- Bet-Ha'emek, 13- Zonem, 14- Meron, 15- Gilon, 16- Esh'har, 17- Hilazon, 18- Sha'abi, 19- Hararit, 20- Azmon, 21- Nazerat, 22- Tavor, 23- Givat-Hamore, 24- Peqi'in, 25- Kisra, 26- Livnim, 27- Nahef. (Shaded relief map: by Hall, 1993)

All these studies show that simple analysis of selected morphometric parameters enable to reconstruct the age and nature of tectonism, that shaped the present morphology, and to generate a regional model for the geomorphic response to large scale tectonic activity.

In this study we present a new method, which applies morphometric analysis to determine the relative age of tectonic escarpments in the Galilee. Age constraints on this relative sequence are obtained by comparing undated tectonic escarpments with a tectonic escarpment of known age.

Slope evolution in the Galilee since the Plio-Pleistocene are dominated by karstic activity. Mass wasting processes are minor. Furthermore, morphologic features developed through the reduction of material by dissolution, preventing the formation of sediment-dependent landforms such as fluvial terraces and alluvial fans.

## 3. Geographic and Geologic Setting

The Galilee is situated in northern Israel between the Mt. Carmel in the south and southern Lebanon in the north (Fig. 1). It is divided along the Zurim escarpment into the Lower and Upper Galilee. The Lower Galilee consists of a series of east-west oriented tectonic ridges bounded by normal faults (Freund, 1970) and separated by elongated valleys. The average altitude of the ridge crests is 500 meters asl. The Upper Galilee is higher than the Lower Galilee with its highest summit located at 1200 meters asl. The Galilee is crossed by a series of NW-SE oriented left-lateral faults and NE-SW oriented right-lateral faults (Ron et al., 1984). Several of these faults curve and become EW normal faults (Ron et al., 1984). Most of the topographic expression of this fault system has been eroded. In both the Upper and Lower Galilee there is evidence for fold structures that developed during the Late Cretaceous (Flexer et al., 1970).

The mountainous backbone of the Galilee is composed mainly of limestone and dolomite of Cenomanian and Turonian age (Picard and Golani, 1965). A lower Cretaceous sequence of marls, sandstone and limestone is exposed in several locations, such as at the Zurim and Ramim escarpments (Fig. 1) (Eliezri, 1965; Golani, 1957). Senonian and Eocene chalk and limestone are exposed along the margins of the

mountains and in the Nahal Dishon area (Shlein, 1961; Kafri, 1972). Three main processes determine the extent of the present rock exposure: (1) the structural relief of the pre-Eocene anticlines and synclines of the Syrian Arc fold belt (2) the degree of truncation that took place after the regression of the Eocene sea and (3) Plio-Pleistocene tectonic deformation.

The climate in the mountainous areas of the Galilee is of a Mediterranean type , with dry summers and rainy winters. Annual precipitation ranges between 600-1000 mm, with an average of 700-800 mm over most of the area.

## 4. Erosion of Landforms in the Galilee

Prior to the tectonic phase that formed the morphotectonic landscape of the Galilee, an erosional surface dominated the landscape of northern Israel, as part of a regional peneplain (Garfunkel, 1988). It is essential to understand the nature of erosion in such a terrain and the relation between rates of denudation and tectonic uplift to follow the morphotectonic evolution of the Galilee.

Several studies have estimated rates of denudation at various scales, using different methods:

* River-load method: measuring sediment load of drainage channels and dividing by the drainage basin area (Einsele and Hinderer, 1998).

* Sediment-budget method: calculating mean denudation rates from the mass accumulated in adjacent basins (Einsele, 1992).

* Determining chemical denudation rates from mass balances of soil profiles and total dissolved materials in river runoff and springs (Gerson, 1976; Retallack, 1990; Atkinson and Smith, 1978; Jennings, 1971; Trudgill, 1985;).

Ahnert (1970) used denudation rates of 20 rivers to calculate the relation between relief and denudation on a global scale. According to his calculations, the denudation rate over a mean relief of 400 meters is between 30 to 50 m/My. Einsele and Hinderer (1998) present denudation rate values corresponding to various climatic and relief conditions. For low-to-medium relief and semi-arid to temperate climates, they estimate overall denudation rates of 30 to 60 m/My; however, Ritter et al. (1995) estimated denudation rates in the eastern Mediterranean (using data from Walling,

1987) of 20m/My. Considering large drainage basins of thousands to millions of $km^2$, Strahler and Strahler (1992) anticipate that over a mean relief of 300 meters the mean denudation rate should be about 40 m/My. For Israel, Begin and Zilberman (1997) calculated mean denudation rates since the Miocene to be 20 m/My.

The denudation rates presented above cannot explain the difference between the total vertical displacement and the topographic height along most of the Galilee escarpments. Furthermore, these denudation rates are based on drainage systems ranging in size from hundreds to millions of $km^2$, mainly in areas of siliceous bedrock where runoff is much higher than on carbonate rocks which is the main lithology over in the Galilee. These rates do not distinguish between rates of stream incision, slope erosion, and mountaintop lowering. Ahnert (1970) argues that in an extensively flat landscape dissected by streams, such as the upper surfaces of the uplifted blocks in the Galilee, the main part of the sediment load is derived from the slopes whereas little or nothing is contributed from the interfluves. Bierman et al. (1995) calculated erosion rates of granitic domes that range between 2 to 10 m/My. Bierman and Turner (1995) calculated erosion rates as low as 0.7 m/My in Australia by measuring the concentration of cosmogenic $^{10}Be$ and $^{26}Al$ upon isolated inselbergs. The results that were obtained by using cosmogenic isotope concentration demonstrate the very low erosion rates of lifted morphologic elements that are not subjected to intense alluvial processes.

The evolution of the drainage network over most of the Galilee, recently composed of short and low energy drainage channels, was controlled by the development of two large-scale tectonic features:

A) The Dead Sea Rift Valley, which cut the Mediterranean watershed from its eastern drainage area and thus reduced significantly the size of the drainage systems that flow westward across the Galilee. The formation of the Dead Sea Rift Valley initially started about 8 Ma a, and became the main controlling factor in the shaping of the morphology of the area during the Late Pliocene (Shaliv, 1991).

B) The Late Pliocene and Pleistocene arching of the Galilee (Picard, 1943; Matmon et al., in press) established the regional water divide between the Dead Sea Rift Valley and the Mediterranean and led to an additional decline in the watershed of the west-flowing streams in the Galilee.

The denudation values obtained by Begin and Zilberman (1997) are mean denudation rates corresponding to a long period and do not account for short time variations triggered by rapid tectonic activity of sea-level fluctuations. Decreased denudation rates resulting from the significant reduction in the area of the drainage system in the area in the last 2 million years are not accounted for as well.

Lowering of carbonate surfaces by chemical processes in climates similar to the Galilee climate is estimated to range between 20 to 40 m/My (Atkinson and Smith, 1978; Jennings, 1971; Trudgill, 1985; Bloom; 1991). Therefore, the actual surface lowering rates of the uplifted blocks of the Galilee probably do not exceed 20 m/My.

This value is firmly supported by the preservation of uplifted ancient surfaces in Israel, sometimes capped by Miocene sediments. The uniformity of exposed rock formations along the ridge tops and lack of incision into older and deeper strata and the maintenance of flat ridge tops manifest the lack of alluvial activity on the upper surface. The stability of the upper surfaces of the tectonic blocks in the Galilee (see discussion of the history of the Tur'an block) indicates that elevated morphotectonic features were not subjected to intensive erosion during Plio-Pleistocene times.

## 5. Geomorphic Parameters

The morphology of the Galilee escarpments is described semi-quantitatively by two parameters: the L-index value parameter and the degree of concavity of undated tectonic slopes compared to a tectonic slope of known age.

### 5.1 The L-index Value

#### *5.1.1 The concept*

The L-index is a dimensionless parameter that expresses the ratio between the height of an escarpment (i.e., the topographic difference between the base and the top of the escarpment) and the total vertical displacement (Fig. 2). Therefore, L-index

$$L = \frac{\text{Height of escarpment}}{\text{Total stratigraphic displacement (top of Bina Fm.)}}$$

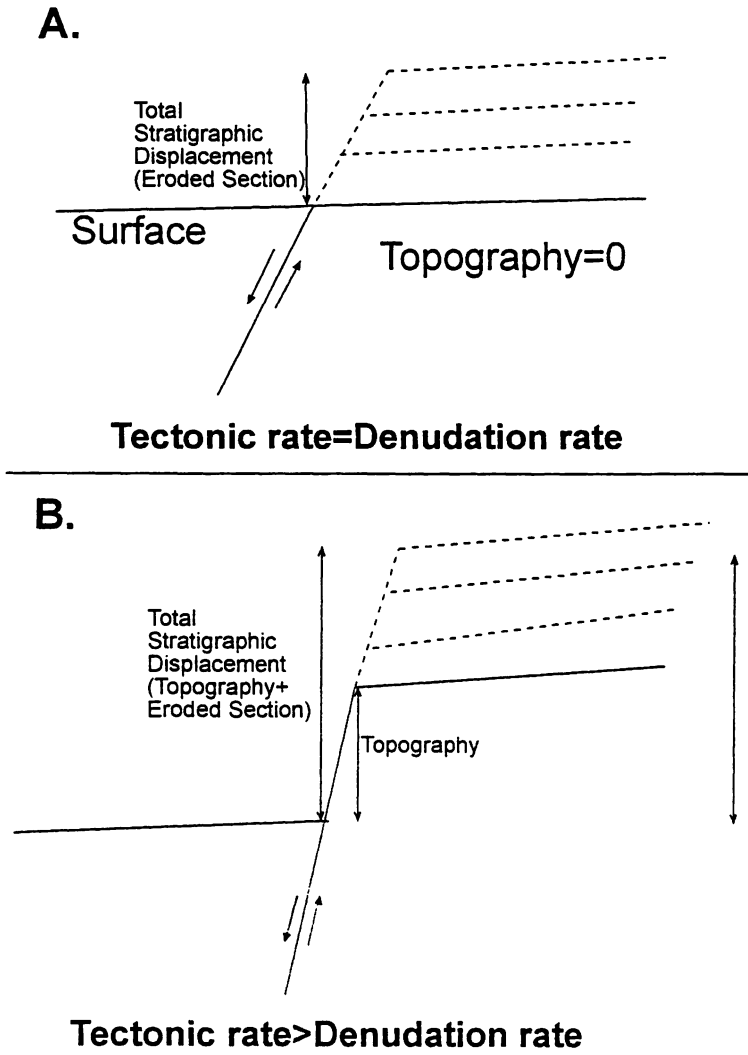


Fig. 2- The L-index concept. (a) Vertical displacement with no topographic expression; the ratio between topography and vertical displacement is zero. This situation occurs when the rate of vertical displacement does not exceed the rate of denudation. (b) Vertical uplift rate is greater than the rate of denudation and topography forms; the ratio between topography and vertical displacement ranges between zero and one.

values should range between zero and one. Low L-index values indicate that most of the topographic expression of the tectonic displacement was eroded. Such values characterize faults that their rate of displacement was equal or less than the rate of denudation, and therefore, have no topographic expression. High L-index values indicate that most of the tectonic displacement is expressed as morphostructural relief indicating that the rate of vertical uplift exceeded denudation rate. Intermediate L-index values indicate that a portion of the total uplift was eroded. The question is when did the erosion occur.

Considering the nature of erosion and surface lowering in the Galilee discussed above, we can assume that the missing portion of the sequence along the Galilee escarpments was stripped away during a time of slow uplift rates. Topographic expression was formed later when the rate of tectonic uplift exceeded the rates of erosion. The summits of the uplifted blocks became local water divides, subjected to minor erosion and therefore, their initial topography was preserved. This implies that the L-index value reflects the tectonic history of the vertical displacement along a fault indicating an initially low rate tectonic activity, followed by a rapid relief-forming phase.

### *5.1.2 L-index value calculation procedure*

Topographic data were obtained from Digital Terrain Modeling (D.T.M.) of Israel (Hall, 1993). Structural contours were compiled from structural maps of the Galilee (Kafri, 1972; Levy, 1983; Eliezri, 1965; Saltzman, 1964; Bein, 1967; Glikson 1965; and Cohen, 1988). Since the structural contour is 50 m and only major morphologic features (scale of hundreds of meters) are considered, the analysis ignores the effect of minor tectonic elements and local erosion. These two data sets were combined with Geographical Information Systems (GIS) to calculate L-index values at several points along each escarpment in the study area. Interpolation of L-index values between the points along an individual fault line were carried out by GIS (Hebrew University). The results are separated into three groups indicating low (0-0.25), intermediate (0.25-0.75) and high (0.75 and higher) values. In practice, values higher than 1 are possible. These values result from the uncertainty in the determination of the topographic and structural elevations (see L-index value sensitivity test). Therefore,

values that range between 1 and 1.1 are considered in the high group values. L-index values above 1.1 were not considered.

A sensitivity test was carried out to estimate the influence of uncertainty on the various parameters used to determine the L-index value. We assume that the main error in calculating the L-index value arises from contour-line interpolation in topographic and structural maps. The maximum error estimated for the topographic elevation is ±10 m and for the structural elevation is ±50 m. This yields a maximum error estimate for the topographic and structural differences across a fault of ±20 m and ±100 m, respectively. The calculation of extreme L-index values by using negative and positive maximum error are presented in Table 1. Maximum L-index value is calculated by dividing the largest possible topographic difference across a fault by the smallest structural difference. Minimum L-index value is calculated by dividing the smallest possible topographic difference by the largest possible structural difference. It can be seen that the largest value calculated is 3.07. As discussed above, L-index values should not be greater than 1, therefore the maximum topographic and structural errors are overestimated. They are thus reduced to yield a maximum L-index value of one. Therefore, the maximum error in topographic values is reduced to ±3.125 m and the maximum error in structural values is reduced to ±16.125 m (Table 1). The reduced uncertainty values cause negligible changes in the L-index value calculated on escarpments higher than 200 meters. Since most of the analyzed escarpments are higher than 200 meters their corresponding L-index values are not influenced by the measurement error.

### *5.1.3 Results*

L-index values were calculated along most of the escarpments in the Galilee (Table 2). Values range between –0.146 and 8.115. Extreme values (lower than 0 and higher than 1.1) result from a local complex structure that does not allow the determination of adequate points for L-index value calculation. Results are displayed graphically on a fault line map. An example of such display is shown in Figure 3. Low L-index values, which indicate a long period of a slow activity rate generally

**Table 1 - Sensitivity test for the L-value calculation**

| Location | difh 1) | difs 2) | L-value | lower error bar difh | lower error bar difs | Min. L-value | upper error bar difh | upper error bar difs | Max. L-value |
|---|---|---|---|---|---|---|---|---|---|
| Bet-Haemek | | | | | | | | | |
| 1.00 | -50.88 | -134.45 | 0.38 | -30.88 | -234.45 | 0.13 | -70.88 | -34.45 | 2.06 |
| 2.00 | -98.90 | -138.73 | 0.71 | -78.90 | -238.73 | 0.33 | -118.90 | -38.73 | 3.07 |
| 3.00 | -115.15 | -157.19 | 0.73 | -95.15 | -257.19 | 0.37 | -135.15 | -57.19 | 2.36 |
| 4.00 | -115.30 | -169.07 | 0.68 | -95.30 | -269.07 | 0.35 | -135.30 | -69.07 | 1.96 |
| 5.00 | -135.75 | -385.37 | 0.35 | -115.75 | -485.37 | 0.24 | -155.75 | -285.37 | 0.55 |
| 6.00 | -106.43 | -346.25 | 0.31 | -86.43 | -446.25 | 0.19 | -126.43 | -246.25 | 0.51 |
| 7.00 | -145.18 | -348.55 | 0.42 | -125.18 | -448.55 | 0.28 | -165.18 | -248.55 | 0.66 |
| Rosh-Haniqra | | | | | | | | | |
| 8.00 | -121.63 | -673.00 | 0.18 | -101.63 | -773.00 | 0.13 | -141.63 | -573.00 | 0.25 |
| 9.00 | -223.50 | -769.00 | 0.29 | -203.50 | -869.00 | 0.23 | -243.50 | -669.00 | 0.36 |
| 10.00 | -295.35 | -798.00 | 0.37 | -275.35 | -898.00 | 0.31 | -315.35 | -698.00 | 0.45 |
| 11.00 | -273.53 | -811.00 | 0.34 | -253.53 | -911.00 | 0.28 | -293.53 | -711.00 | 0.41 |
| Har-Haluz | | | | | | | | | |
| 12.00 | -335.68 | -440.00 | 0.76 | -315.68 | -540.00 | 0.58 | -355.68 | -340.00 | 1.05 |
| 13.00 | -286.35 | -355.00 | 0.81 | -266.35 | -455.00 | 0.59 | -306.35 | -255.00 | 1.20 |
| Kishor | | | | | | | | | |
| 14.00 | -166.00 | -302.42 | 0.55 | -146.00 | -402.42 | 0.36 | -186.00 | -202.42 | 0.92 |
| 15.00 | -264.98 | -293.25 | 0.90 | -244.98 | -393.25 | 0.62 | -284.98 | -193.25 | 1.47 |
| 16.00 | -261.44 | -309.36 | 0.85 | -241.44 | -409.36 | 0.59 | -281.44 | -209.36 | 1.34 |
| 17.00 | -238.74 | -320.53 | 0.74 | -218.74 | -420.53 | 0.52 | -258.74 | -220.53 | 1.17 |
| Zonem | | | | | | | | | |
| 18.00 | -197.75 | -250.00 | 0.79 | -177.75 | -350.00 | 0.51 | -217.75 | -150.00 | 1.45 |
| 19.00 | -194.45 | -256.38 | 0.76 | -174.45 | -356.38 | 0.49 | -214.45 | -156.38 | 1.37 |
| 20.00 | -167.95 | -235.00 | 0.71 | -147.95 | -335.00 | 0.44 | -187.95 | -135.00 | 1.39 |

Error correction assumes contour lines are in place.
Error is atributed to interpulation only.
Max. error on structural height is 50 meters; therefore, max. error of difs is 100m
Max. error on topographic height is 10 meters; therefore max. error of dift is 20m.
L-value cannot be higher than 1, therefore errors must be smaller than
max. assumed.
The 2nd cross section of the Beit Haemek fault has the
largest upper error bar. Therefore, max. errors must be reduced
so the L-value of the 2nd cross section equals 1.
The reduced max. errors are:
16.625m for structural values and 3.325m for topographic values.
For more details, see text
difh - elevation difference between base and top of escarpment.
difs - vertical displacement.

**Table 1 – An example of the sensitivity test for the calculation of L-value.**

1) difh – elevation difference between base and top of escarpment.

2) difs – vertical displacement.

The second L-index value on the Bet-Ha'emeq escarpment displays the highest value (3.07) when it is calculated using maximum topographic and structural errors. Since, theoretically, L-index value cannot be greater than 1, the assumed errors must be reduced so that calculated L-index value using maximum topographic and structural errors, does not exceed 1. Accordingly, the maximum topographic error is ±3.325m and the maximum structural error is ±16.625m.

# Table 2

**Table 2 L-index values**

| coor1(x) | coor1(y) | topo1 (m) | struct1 (m) | coor2(x) | coor2(y) | topo2 (m) | struct2 (m) | dif-topo (m | dif-struct (m) | mana | |
|---|---|---|---|---|---|---|---|---|---|---|---|
| Nahariyya-Idmit | | | | | | | | | | | |
| 172400 | 1273500 | 370 | 410 | 172700 | 1275200 | 430 | 475 | 60 | 65 | 0.923077 | |
| 171500 | 1274200 | 340 | 420 | 172000 | 1275500 | 440 | 450 | 100 | 30 | 3.333333 | |
| 170000 | 1274200 | 265 | 320 | 170000 | 1276000 | 470 | 470 | 205 | 150 | 1.366667 | |
| 168900 | 1274700 | 210 | 200 | 169100 | 1276100 | 442 | 440 | 232 | 240 | 0.966667 | |
| 167400 | 1274600 | 165 | 100 | 167400 | 1276300 | 320 | 240 | 155 | 140 | 1.107143 | |
| 166500 | 1275200 | 85 | 0 | 166500 | 1277000 | 340 | 225 | 255 | 225 | 1.133333 | |
| 165500 | 1275000 | 65 | -50 | 165500 | 1276900 | 250 | 160 | 185 | 210 | 0.880952 | |
| Nahariyya-Yanuh | | | | | | | | | | | |
| 171300 | 1264500 | 310 | 325 | 171100 | 1265050 | 400 | 660 | 90 | 335 | 0.268657 | |
| 172000 | 1264400 | 370 | 340 | 172000 | 1265200 | 510 | 690 | 140 | 350 | 0.4 | |
| 173000 | 1263750 | 420 | 425 | 173050 | 1265300 | 560 | 715 | 140 | 290 | 0.482759 | |
| 173600 | 1263600 | 435 | 475 | 173600 | 1264800 | 560 | 725 | 125 | 250 | 0.5 | |
| 175800 | 1263200 | 585 | 625 | 176000 | 1264800 | 690 | 775 | 105 | 150 | 0.7 | |
| 176400 | 1262900 | 600 | 625 | 177000 | 1264600 | 695 | 750 | 95 | 125 | 0.76 | |
| 176800 | 1262500 | 630 | 640 | 177500 | 1264300 | 700 | 725 | 70 | 85 | 0.823529 | |
| Nahariyya-Yarka | | | | | | | | | | | |
| 171500 | 1262400 | 410 | 400 | 171500 | 1263600 | 315 | 330 | -95 | -70 | 1.357143 | |
| 172500 | 1262350 | 500 | 620 | 172500 | 1263600 | 390 | 375 | -110 | -245 | 0.44898 | |
| 173100 | 1262200 | 530 | 640 | 173100 | 1263750 | 420 | 450 | -110 | -190 | 0.578947 | |
| 173600 | 1262150 | 550 | 675 | 173700 | 1263600 | 440 | 475 | -110 | -200 | 0.55 | |
| 174350 | 1261900 | 535 | 720 | 174800 | 1262800 | 480 | 575 | -55 | -145 | 0.37931 | |
| 175050 | 1260700 | 585 | 725 | 175800 | 1261600 | 465 | 520 | -120 | -205 | 0.585366 | |
| Nahariyya-Bet-Haemek (north) | | | | | | | | | | | |
| 165000 | 1265500 | 60.825 | 1.179 | 165000 | 1266000 | 111.7 | 135.631 | -50.875 | -134.452 | 0.378388 | |
| 166000 | 1265500 | 79.55 | 65.49 | 166000 | 1266000 | 178.45 | 204.216 | -98.9 | -138.726 | 0.712916 | |
| 167000 | 1265400 | 111.225 | 91.511 | 167000 | 1266300 | 226.375 | 248.704 | -115.15 | -157.193 | 0.732539 | |
| 168000 | 1265500 | 135.85 | 130.606 | 168000 | 1266200 | 251.15 | 299.676 | -115.3 | -169.07 | 0.681966 | |
| 169500 | 1265000 | 200.775 | 214.629 | 170000 | 1265500 | 336.525 | 600 | -135.75 | -385.371 | 0.352258 | * |
| 171200 | 1264500 | 302.275 | 300.389 | 171200 | 1265200 | 408.7 | 646.636 | -106.425 | -346.247 | 0.307367 | |
| 172500 | 1264200 | 376.15 | 366.344 | 172500 | 1265300 | 521.325 | 714.892 | -145.175 | -348.548 | 0.416514 | |
| Nahariyya-Rosh-Haniqra | | | | | | | | | | | |
| 161000 | 1276500 | 30.125 | -300 | 161000 | 1277650 | 151.75 | 373 | -121.625 | -673 | 0.180721 | * |
| 162000 | 1276400 | 55.85 | -300 | 162000 | 1277600 | 279.35 | 469 | -223.5 | -769 | 0.290637 | * |
| 163000 | 1276200 | 41.35 | -300 | 163000 | 1277500 | 336.7 | 498 | -295.35 | -798 | 0.370113 | * |
| 164000 | 1276500 | 86.35 | -300 | 164000 | 1277500 | 359.875 | 511 | -273.525 | -811 | 0.337269 | * |
| Nahariyya-Har-Haluz | | | | | | | | | | | |
| 179500 | 1260700 | 391.675 | 350 | 179500 | 1261600 | 727.35 | 790 | -335.675 | -440 | 0.762898 | * |
| 178700 | 1260600 | 433.65 | 420 | 178700 | 1261300 | 720 | 775 | -286.35 | -355 | 0.80662 | * |
| Nahariyya-Kishor | | | | | | | | | | | |
| 178500 | 1260030 | 278.93 | 140 | 178500 | 1260600 | 444.925 | 442.421 | -165.995 | -302.421 | 0.548887 | |
| 177500 | 1260030 | 262.945 | 220 | 177500 | 1260600 | 527.925 | 513.252 | -264.98 | -293.252 | 0.903591 | |
| 176600 | 1260030 | 290.36 | 280 | 176600 | 1260500 | 551.8 | 589.364 | -261.44 | -309.364 | 0.845089 | |
| 176500 | 1260030 | 305.515 | 370 | 175500 | 1260500 | 544.25 | 690.525 | -238.735 | -320.525 | 0.744825 | |
| Nahariyya-Zonem | | | | | | | | | | | |
| 177600 | 1273600 | 449.825 | 440 | 177300 | 1274300 | 647.575 | 690 | -197.75 | -250 | 0.791 | * |
| 178300 | 1274000 | 465.575 | 453.618 | 178000 | 1274600 | 660.025 | 710 | -194.45 | -256.382 | 0.758439 | * |
| 179100 | 1274300 | 470.975 | 490 | 178500 | 1275300 | 638.925 | 725 | -167.95 | -235 | 0.714681 | * |
| | | | | | | | | | | | |
| Shefar'am- Tuval | | | | | | | | | | | |
| 174500 | 1258800 | 220.075 | 342.281 | 173950 | 1259500 | 570.675 | 701.676 | 350.6 | 359.395 | 0.975528 | |
| 173300 | 1258400 | 220.275 | 250 | 173000 | 1259200 | 516.8 | 703.848 | 296.525 | 453.848 | 0.653358 | |
| 172300 | 1258200 | 210 | 250 | 172000 | 1259200 | 464.65 | 480 | 254.65 | 230 | 1.107174 | * |
| Shefar'am-KKL(gamal) | | | | | | | | | | | |
| 169800 | 1257200 | 108.275 | 110 | 169800 | 1258000 | 230 | 125 | 121.725 | 15 | 8.115 | * |
| 169300 | 1257500 | 100 | 100 | 169300 | 1258100 | 241.25 | 120 | 141.25 | 20 | 7.0625 | * |
| 168500 | 1257700 | 65.7 | 81.486 | 168500 | 1258200 | 189.425 | 115.784 | 123.725 | 34.298 | 3.607353 | |
| 167000 | 1257800 | 39 | -147.526 | 167000 | 1258200 | 112.275 | 20 | 73.275 | 167.526 | 0.437395 | * |
| Shefaram-Ahi'hud | | | | | | | | | | | |
| 170000 | 1256400 | 29.7 | -145 | 170000 | 1256900 | 120.9 | 90 | 91.2 | 235 | 0.388085 | * |
| 169250 | 1256000 | 23.7 | -160 | 169250 | 1256600 | 112.025 | 50.494 | 88.325 | 210.494 | 0.419608 | |
| 167100 | 1256100 | 81.7 | -130 | 167200 | 1256700 | 70 | -50 | -11.7 | 80 | -0.14625 | * |
| Shefar'am-Sha'abi | | | | | | | | | | | |
| 179300 | 1249600 | 330 | 525 | 178600 | 1249100 | 557.9 | 745.99 | 227.9 | 220.99 | 1.031268 | |
| 177500 | 1250400 | 350 | 500 | 177150 | 1249600 | 541.95 | 615.285 | 191.95 | 115.285 | 1.665004 | |
| Shefar'am-Esh'har | | | | | | | | | | | |
| 178800 | 1253700 | 279.8 | 469.812 | 178600 | 1254500 | 381.175 | 525.465 | 101.375 | 55.653 | 1.821555 | |
| 178200 | 1253200 | 250.425 | 326.568 | 177900 | 1254200 | 361.375 | 453.423 | 110.95 | 126.855 | 0.874621 | |
| 177500 | 1253300 | 200 | 200 | 177200 | 1253900 | 319.3 | 393.567 | 119.3 | 193.567 | 0.616324 | |
| Shefar'am-Gilon | | | | | | | | | | | |
| 170900 | 1256000 | 29.65 | -110 | 170900 | 1257000 | 169.75 | 173.424 | 140.1 | 283.424 | 0.494312 | |
| 171800 | 1255600 | 30.3 | -70 | 172400 | 1256700 | 360 | 308.781 | 329.7 | 378.781 | 0.870424 | |
| 173200 | 1255500 | 40.175 | -30 | 173200 | 1256500 | 326.075 | 325.421 | 285.9 | 355.421 | 0.804398 | |
| 174000 | 1255500 | 56.775 | 10 | 174000 | 1256400 | 366.725 | 362.629 | 309.95 | 352.629 | 0.878969 | |
| 174800 | 1255650 | 175.65 | 96.342 | 174800 | 1256050 | 310.025 | 355.796 | 134.375 | 259.454 | 0.517915 | |
| Shefar'am-Azmon | | | | | | | | | | | |
| 177000 | 1246000 | 149.075 | -50 | 177000 | 1247400 | 425.925 | 561.868 | 276.85 | 611.868 | 0.452467 | |
| 176000 | 1246400 | 160.9 | -25 | 176000 | 1247400 | 478.1 | 646.209 | 317.2 | 671.209 | 0.47258 | |
| 175300 | 1246400 | 167.3 | 0 | 175300 | 1247600 | 514.175 | 702.994 | 346.875 | 702.994 | 0.493425 | |
| 174000 | 1246400 | 176.35 | 20 | 174000 | 1247400 | 400.775 | 601.828 | 224.425 | 581.828 | 0.385724 | |
| 172950 | 1246000 | 218 | 30 | 172950 | 1247050 | 345.925 | 478.274 | 127.925 | 448.274 | 0.285372 | |
| Shefar'am-Qoranit | | | | | | | | | | | |
| 174400 | 1250600 | 340 | 290 | 174000 | 1250000 | 459.125 | 530.063 | 119.125 | 240.063 | 0.496224 | |
| 173800 | 1250900 | 320 | 240 | 173500 | 1250400 | 450.275 | 500 | 130.275 | 260 | 0.501058 | * |
| 173100 | 1252200 | 260 | 180 | 172600 | 1251000 | 391.025 | 439.489 | 131.025 | 259.489 | 0.504935 | |
| 172500 | 1252500 | 230 | 170 | 172000 | 1251600 | 351.375 | 399.666 | 121.375 | 229.666 | 0.528485 | |

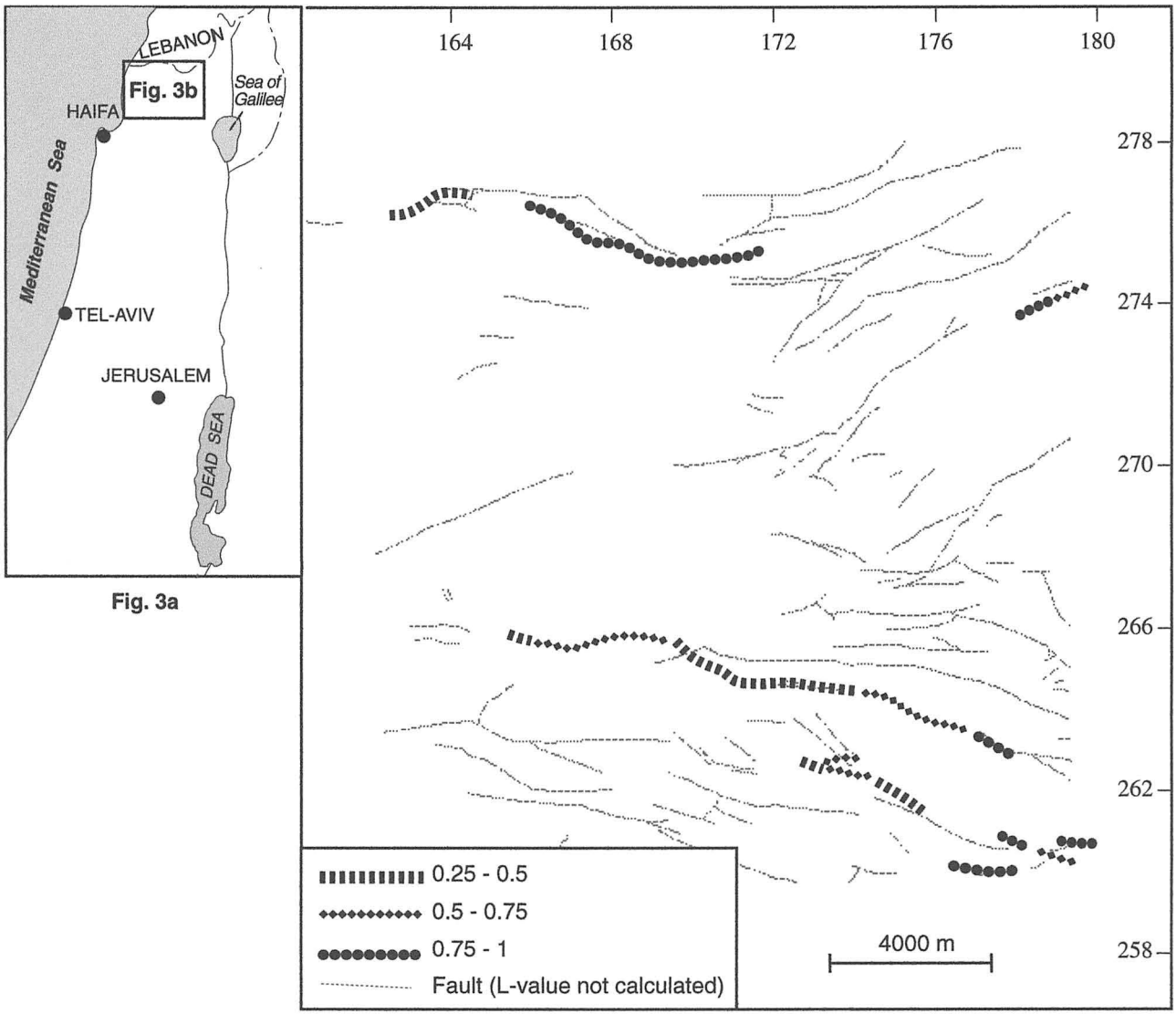


Fig. 3a

Fig. 3b

Fig. 3 –Example of L-index value calculation along escarpments in the northwestern part of the Galilee. Most of the faults do not form topography.

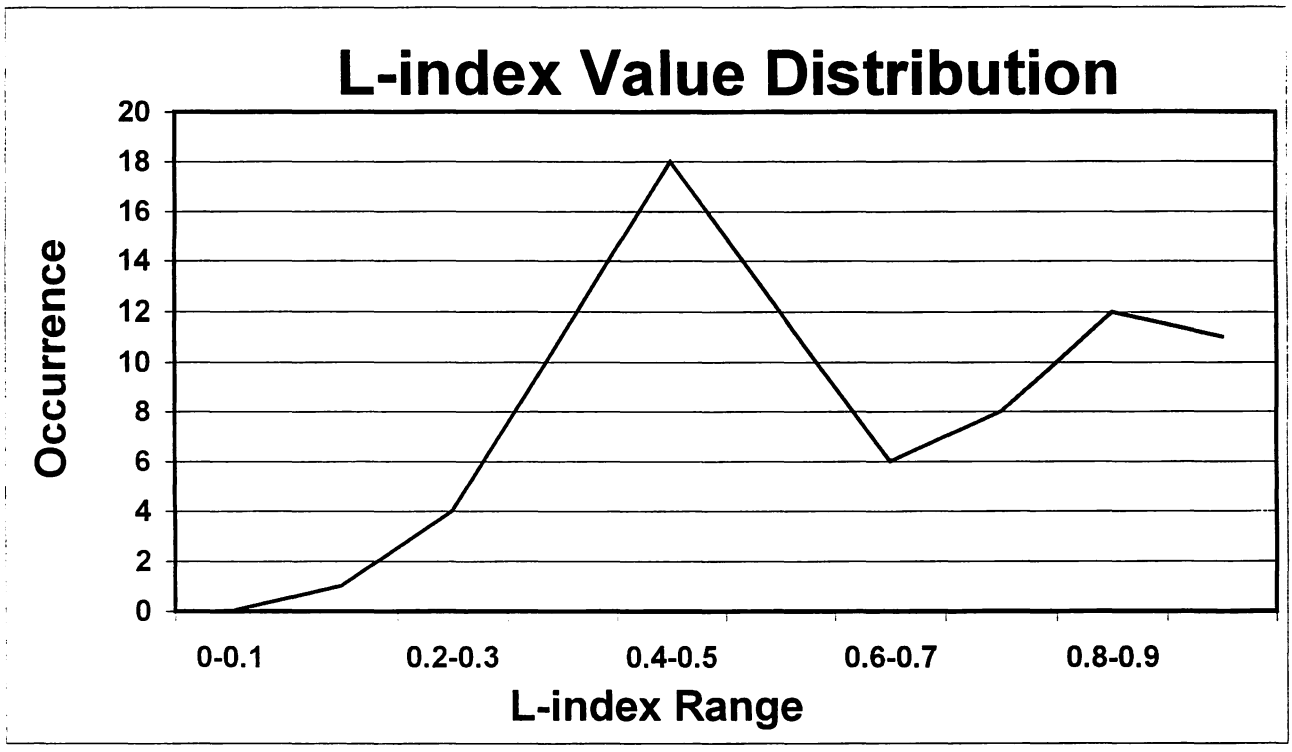


Fig. 4 –Distribution of L-values indicates that the normal faults of the Galilee are divided into two groups that differ in the length of time that they were active under truncation conditions and in the length of high-rate tectonic activity period, when topography was formed.

characterize the main, large escarpments, such as the Zurim and Rosh-Haniqra escarpments (Fig. The L-index values show a bimodal distribution indicating two groups of faults. The first group at 0.4-0.5 and the second group at 0.8 and higher.

### *5.1.4 Discussion and Conclusions*

The accurate calculation of the L-index value is possible due to the widespread occurrence of Mesozoic marine sediments that maintain their thickness and lithology throughout the Galilee. This enables the comparison between the amount of tectonic displacement and its morphologic expression. Since the ratio between tectonic displacement and its morphologic expression is indicative of both tectonics and of surficial processes, the L-index value is a tool in recognizing different tectonic

surficial processes, the L-index value is a tool in recognizing different tectonic segments along a fault line. It also helps to explain variations among tectonic slope profiles when all other parameters (lithology, direction of strike of the fault, face aspect of the slope) of the compared slopes are identical.

The calculation of L-index value along tectonic slopes in the Galilee leads to four principal conclusions:

(1) L-index values vary systematically along some fault lines. This variation indicates the division of the faults into segments, which have a different tectonic history.

(2) Some escarpments such as the Rosh-Haniqra escarpment, were on fault systems that have been active from the onset of extensional deformation in the Galilee in the Miocene (Freund, 1970; Ron et al., 1984) until the Late Pleistocene. The long duration of activity is indicated, on one hand, by the low L-index values and, on the other hand, by morphologic elements indicating Late Pleistocene activity.

(3) Most of the escarpments in the Galilee have intermediate L-index values (0.4-0.5) and do not show evidence of young tectonic activity. The intermediate L-index values and the absence of recent tectonic induced morphologic elements indicate that the majority of the faults in the Galilee were active for a long time at rates compatible with denudation and did not form topography. Tectonic activity has reduced significantly along these faults, after forming the recent topography during the Lower Pleistocene (Matmon et al., in press).

(4) The bimodal distribution of L-index values indicates two groups of faults: one group is characterized by a long period of low-rate vertical displacement under continuous denudation processes, and a second group characterized by a shorter period of low-rate vertical displacement under denudation processes than the first group. A comparison of the slope profiles (as done below) shows that the two groups differ in the time that they formed topography as well as in the length of time that they were active without forming topography.

## 5.2. Shape of Topographic Profiles of Escarpments

### *5.2.1 The Concept*

Field observations (Ahnert, 1973b), conceptual-theoretical models (Davis, 1899; Simons, 1962; King, 1957) and computer models (Ahnert, 1966, 1973a; Hirano, 1968) show that the natural development of slopes is generally from convex to concave. As long as the rate of uplift is higher than the rate of erosion the slope maintains its convex shape. When the rate of tectonic uplift declines the slope gradually becomes concave. Therefore, in a morphotectonic setting that is controlled mainly by time, the degree of concavity is directly related to the age of the escarpment and to the length of time of relative tectonic quiescence (Mayer, 1986). This is the case in the Galilee as well, where the shape of a tectonic slope with a well-preserved fault scarp at their base is generally convex (Fig. 5). The Nahef escarpment is a good example of a young tectonic slope that has been developing since the Middle to Late Pleistocene until recent. The existence of concave slopes in older escarpments indicates that tectonic slopes in the Galilee evolve from a convex to a concave shape. In a carbonate-dominated terrain, such as the Galilee, only a small amount of the material form the upper part of the slope is transported and deposited at the colluvial apron at its base because most of the material is dissolved and transported away mainly through the karstic system. This process dominates the development of slope.

### 5.2.2 *The Reference Slope - Mt. Tur'an*

A comparison of the degree of concavity among slopes was used in the studied region to establish a relative temporal framework for the development of the various escarpments. Nevertheless, absolute time constraints are necessary because slope analysis provides the only reliable means to date tectonic activity in this region. Such constraints are provided by the Tur'an block located in the Lower Galilee (Fig. 1) where the top of the uplifted block and the down faulted block are capped by a 4.23 Ma basalt of the Cover Basalt Formation (Schulman, 1962; Heimann et al., 1996) that covered the pre-erosional surface mentioned above. The total vertical displacement along the Tur'an fault system is 625 m (Freund, 1970). The escarpment is 300 m high.

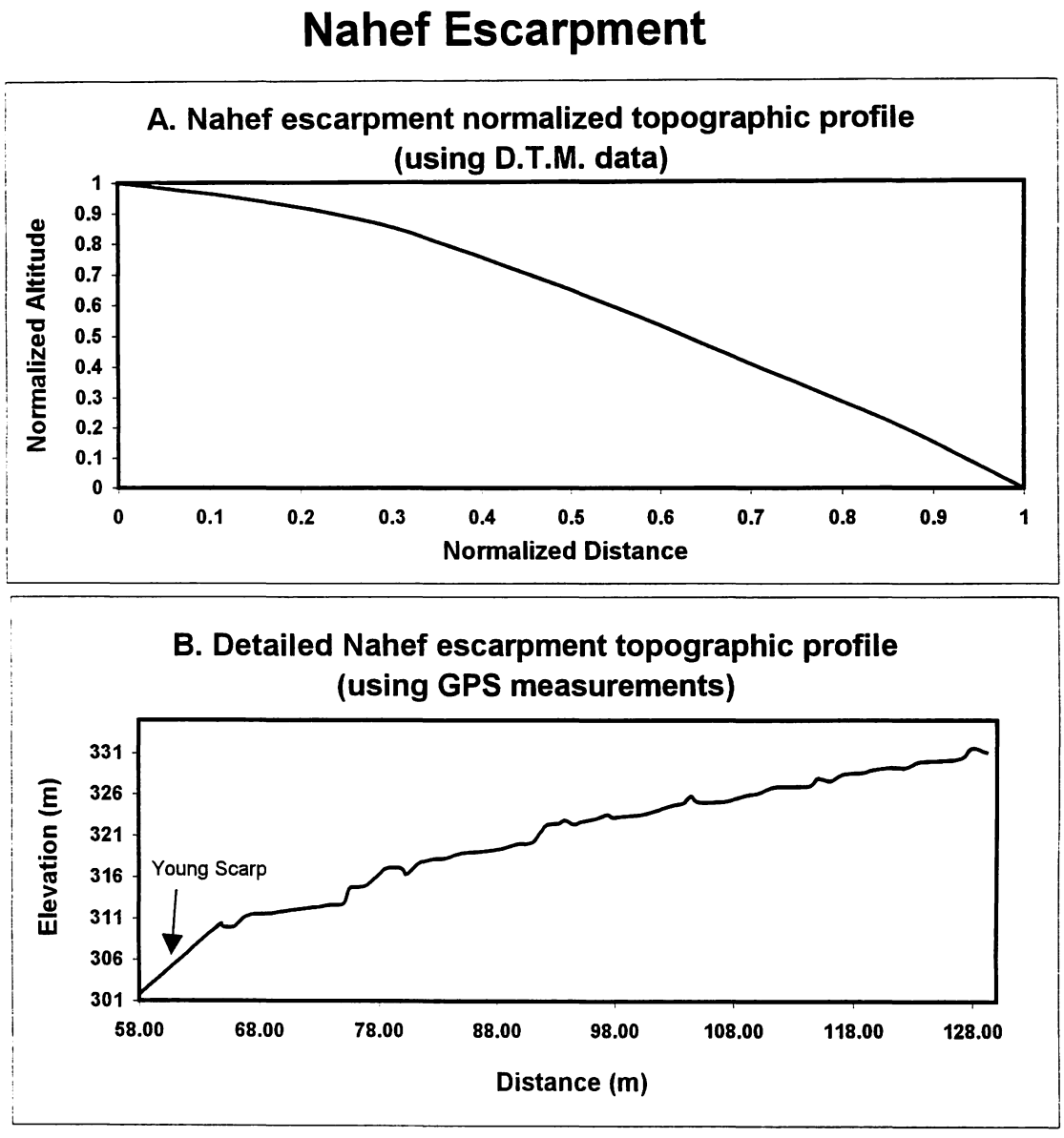


Fig. 5 –Topographic cross-section of the Nahef escarpment. A: A normalized profile using D.T.M. data. The overall shape of the Nahef escarpment is convex even though the resolution of the D.T.M. does not enable the fault scarp at the base of the escarpment to be seen. B: A detailed topographic profile of the Nahef escarpment using GPS measurements. The convex profile and the young fault-scarp at its base are better manifested in a detailed topographic profile of this escarpment. This is a young escarpment with a well preserved fault scarp at its base. The slope has convex shape and is a good example of the initial shape of tectonic slopes in the Galilee.

. The Cover Basaltis displaced by 300 m (Fig. 6; Golani, 1957; Bein, 1967; Ron et al., 1984). Thus, the L-index value of the escarpment is approximately 0.5. As such, the profile of the Tur'an escarpment is the best example of a 4 million year old tectonic escarpment developed in carbonate rocks in a Mediterranean climate, and it can serve as a reference for calibrating the age of the other tectonic escarpments in the Galilee.

### 5.2.3 *The Tur'an Reference Envelope*

Fifteen topographic cross sections of the Tur'an block were constructed (Figs. 7,8). The profiles were constructed along interfluves to avoid the influence of channels. This criterion was used for all the topographic cross sections that were constructed. Fourteen exhibit good similarity (Figs. 7, 8) and are used to calculate a reference envelope (Fig. 9), which allows for natural variation of the slope's shape due to factors such as lithology, escarpment face aspect, and relation of dip direction to face aspect. In places where the escarpment is constructed of a single fault, the profiles include the entire escarpment; in places where the escarpment is composed of several parallel faults, the cross sections include individual faults and the escarpments formed by them (Fig. 7).

### *5.2.4 Profile Comparison Method*

The comparison of different tectonic slopes to the Tur'an reference envelope is restricted to slopes that are: (a) composed of hard carbonate rocks of the Cenomanian and Turonian Judea Group and, (b) not incised by streams at their base.

The degree of influence of lithology on the slope's shape is shown in figures 8, 10A and 10B. Slopes of similar age which are composed of different stratigraphic units within the Judea Group (e.g. the slopes of Mt. Tur'an which cross various Judea Group stratigraphic units) have similar slope profiles (Fig. 8). Therefore, slopes composed of similar lithology but having different profiles are probably of different age (Fig. 10A). Conversely, slopes composed of stratigrapic formations not of the Judea Group have different slope profiles even if they are of similar age. For example, the tectonic escarpment of Haon displaces the Cover Basalt, so its age is similar or

younger to the Tur'an escarpment. Nevertheless, the Haon slope, which is composed of Neogene sediments and volcanic rocks, has a profile which is significantly different from the Tur'an reference envelope (Fig. 10B).

Some of the tectonic escarpments in the Galilee are accompanied by incising streams at their base. Incision of streams at the base of tectonic escarpments significantly influence slope evolution. In such cases, slope evolution is dependent on

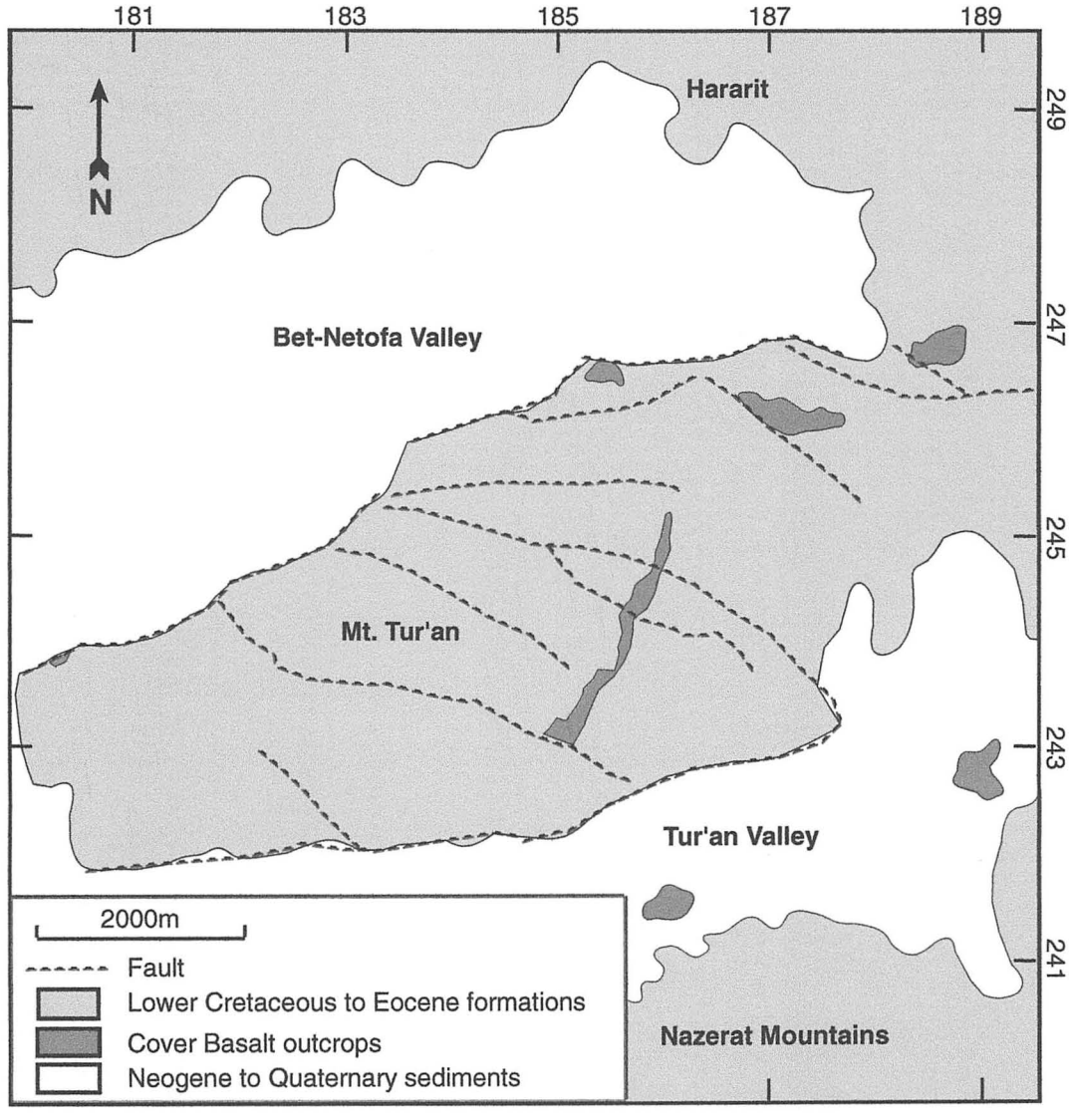


Geology: after Vroman, 1958; Michelson, 1970

Fig. 6 – Geologic map of Mt. Tur'an. The Cover Basalt flowed over a gentle topography that preceded normal faulting and formation of the Tur'an block.

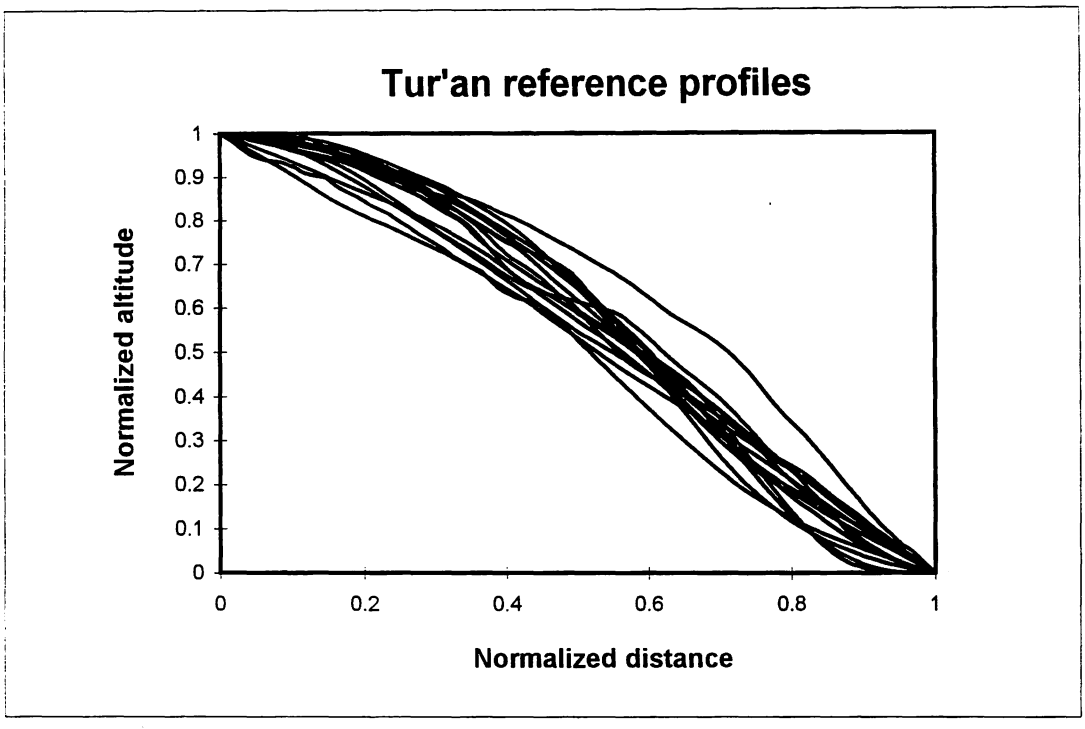


Fig. 7 – The Tur'an reference profiles. Fifteen topographic profiles across the various escarpments of the Tur'an block were plotted. The profiles include all sides of the uplifted block in order to accommodate for natural variations in the profile shapes that result from minor variations in lithology, proximity to drainage channels and face aspect. Generally, the profiles were constructed along interfluves to minimize the influence of active drainage channels on the shape of the slope. Fourteen of the profiles are similar and were used to determine the Tur'an reference envelope (see Fig. 8). All profiles were normalized to allow the comparison of profiles of different height and length.

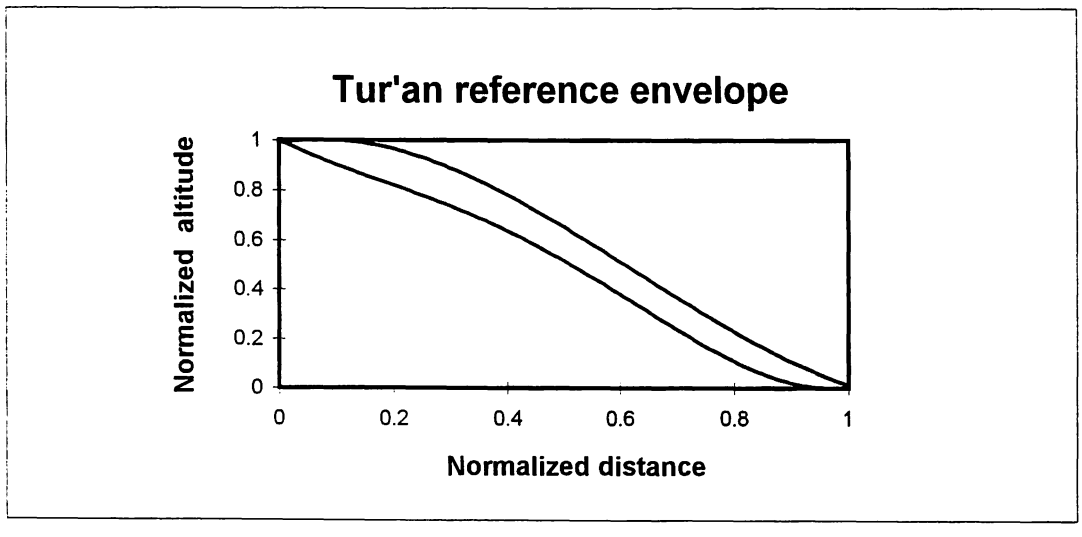


Fig. 8 – The Tur'an reference envelope was determined by digitizing the lower and upper boundaries of the space defined by the topographic profiles (excluding the Tur'an-8 profile)

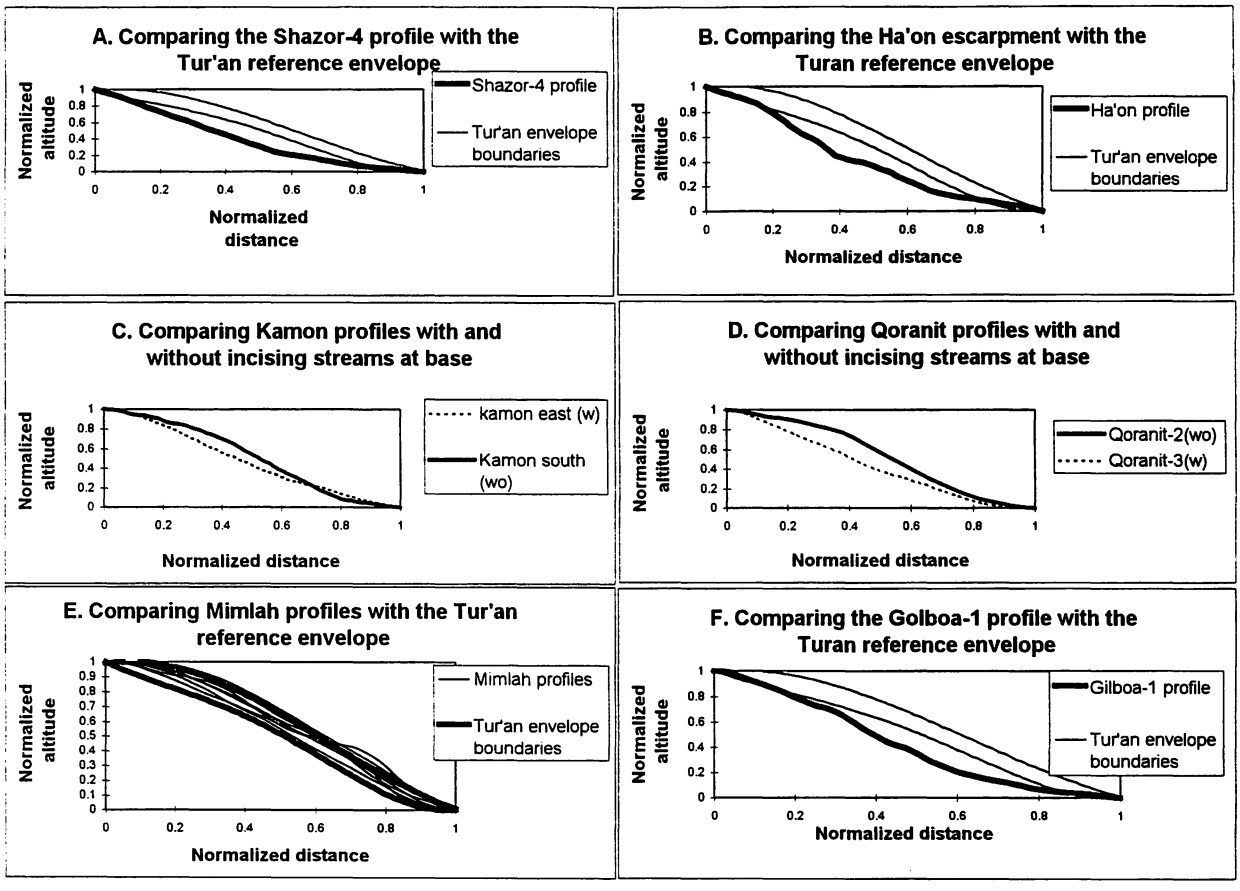


Fig. 9 – (A) Comparison between the Tur'an reference envelope and the Shazor-4 profile. Even though the Shazor-4 slope is composed of a lithological sequence similar to that of the Tur'an escarpment, their slopes have different shapes. (B) Comparison between the Tur'an reference envelope and the Haon escarpment profile, which is composed of Neogene clastic and volcanic rocks. Even though both escarpments displace the Cover Basalt and, therefore, are probably of similar ages, the slope of the Haon escarpment is more concave than the Tur'an reference envelope due to the contribution of mass wasting processes in the development of the Haon escarpment. (C) Comparison between the slope of the southern escarpment of the Kamon block and the slope of the eastern escarpment of the Kamon block where Nahal Zalmon is incised at the base. Dashed line = eastern escarpment with incising stream, solid line = southern escarpment without incising stream. Even though both escarpments are of the same age, the influence of the incising stream on the shape of the slope is evident. The shape of the eastern slope is more concave than the southern one and therefore falsely appears to be older. (D) Comparison between two parts of the Qoranit escarpment demonstrating the influence of stream incision at the base of the escarpment on the shape of the slope. Dashed line = Qoranit-3 profile with incising stream, solid line = Qoranit-2 profile without incising stream. As is the case with the Kamon block (Fig. 8C), the slope with an incising stream at its base

is more concave than the slope without an incising stream at its base; therefore, the former falsely seems to be older. (E) Comparison between the Tur'an reference envelope (defined by thick lines) and the Mimlah profiles. Both sets of escarpments displace basalt flows of similar age and are composed of similar lithology. The Mimlah profiles fit into the Tur'an reference envelope except for the Mimlah-6 profile, which is composed of two parallel normal faults each forming an escarpment that fits into the Tur'an reference envelope. (F) Comparison between the Tur'an reference envelope and the Gilbo'a1 profile. The Gilbo'a1 profile is more concave than the Tur'an reference envelope. The Gilbo'a escarpment displaces a 6 Ma basalt flow and is therefore expected to be older than Tur'an block; thus, its profile is expected to be more concave than the Tur'an reference envelope.

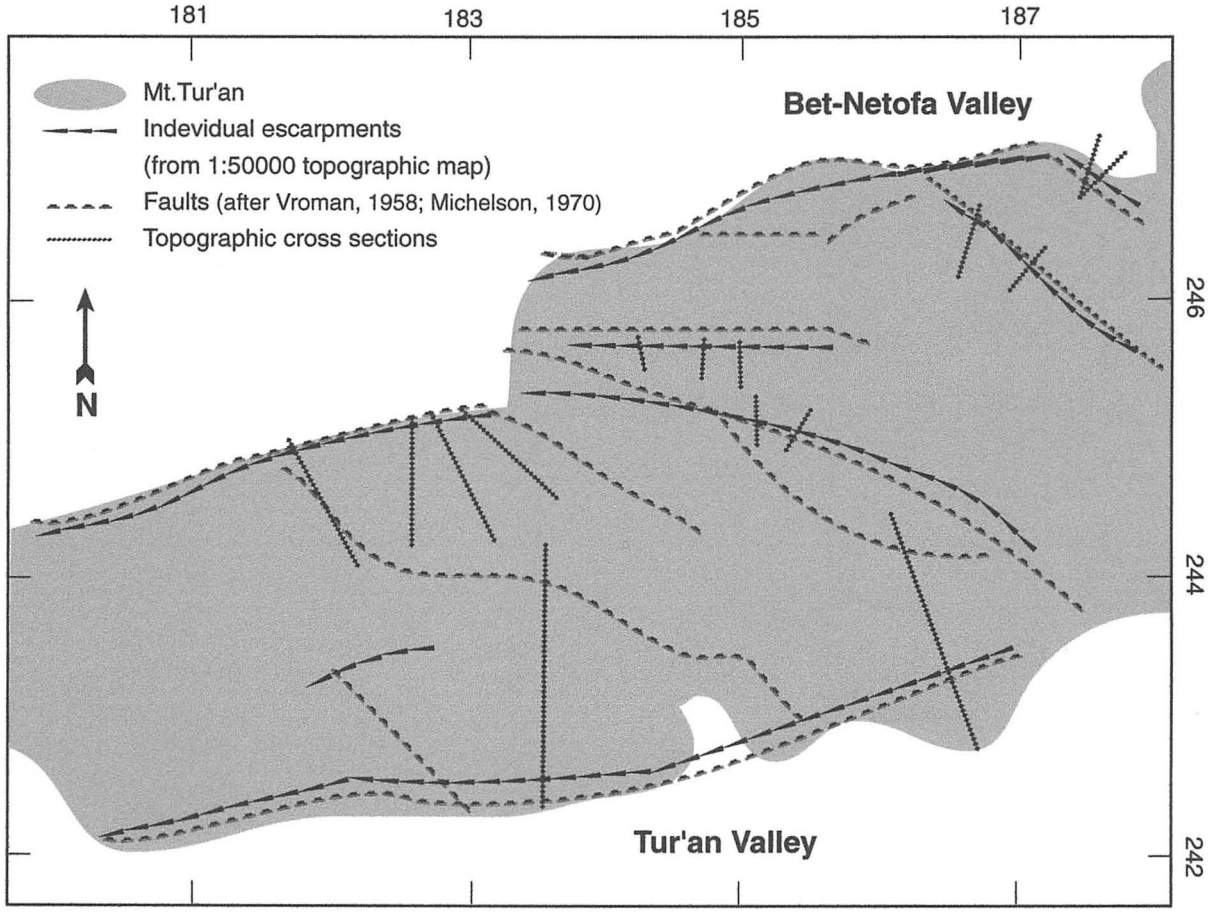


Fig. 10 –Locations of the topographic cross-sections on the Tur'an block. The topographic escarpments generally coincide with the normal faults that cross the block. This agreement is evidence for the morphology of the block being controlled by the distribution and activity of the faults, and not by lithology.

fluvial processes as well as time. The Mt. Kamon and Qoranit escarpments (Fig. 1) can illustrate this case. The summit of Mt. Kamon is situated in the southeastern corner of the Kamon ridge and rises above both the southern and the eastern escarpments. Nahal Zalmon is deeply incised along the eastern escarpment. Even though the stratigraphy and the age of the southern and eastern slopes below the summit are identical (Golani, 1957) the eastern escarpment is mostly concave whereas the southern escarpment is convex (Fig. 10C). This reflects the effect of alluvial processes on the eastern slope. Similarly, Nahal Segev is incised along the base of the Qoranit escarpment. In some places it is incised directly along the fault line and in other places it meanders on the down-faulted block away from the escarpment. Even though the stratigraphy and age along the escarpment remain constant (Kafri, 1965), the slope on the escarpment segments incised by Nahal Segev differ from slopes on the segments where the river does not abut the escarpment (Fig. 10D). In both cases, it is evident that the presence of incising streams leads to the development of concave slopes. Slopes whose evolution is only time-dependent tend towards a more convex shape.

It is possible to test the reliability of slope comparison in two field sites:

(A) The eastern side of the Mimlah escarpment (Fig. 1) is composed of Cenomanian to Turonian limestone and dolomite (Saltzman, 196). Basalts of the Cover Basalt Formation arlocated at the base and on top of the escarpment. The height of the escarpment and the amount of displacement of the Cover Basalt are ~100 m. Seven slope profiles constructed along the Mimlah escarpment are compared to the Tur'an reference envelope (Fig. 10E). Five of the profiles fit within the Tur'an reference envelope. The Mimlah-6 profile has a slight sinusoidal shape and intersects the bottom of the reference envelope. This reflects the presence of two faults, each forming a slightly convex slope and separated by a flat area. The Mimlah-4 profile is slightly more convex than the Tur'an reference envelope. Despite these exceptions, Mimlah escarpment profiles generally fit into the Tur'an reference envelope, which is the expected behavior of escarpments of the same age and similar lithology.

(B) The Gilbo'a escarpment (Fig. 1), which is part of the Carmel fault line, rises 300-400 meters above the Harod Valley and displaces the Intermediate Basalt Formation by about 350 meters. The age of the Intermediate Basalt Formation (~6 Ma; Shaliv, 1991) places a lower limit on the age of the escarpment. An upper limit may be determined by considering the preservation of the Intermediate Basalt on the top of the

uplifted block. This preservation indicates that the topography probably formed a short time after the basalt spilled, securing the basalt from rapid erosion. Therefore, the Gilbo'a escarpment is probably older or similar in age, but definitely not younger, than the Tur'an escarpment. Indeed, the Gilbo'a escarpment exhibits slope profiles significantly more concave than the Tur'an reference envelope (Fig. 10F) indicating that it is older than the Tur'an escarpment. These two case studies are the only other available slopes with information on their age. They demonstrate that the methodology outlined earlier correctly predicts their relative age compared to the Tur'an escarpment.

### 5.2.5 *Results*

Most of the normal faults expressed by topographic escarpments in the order of hundreds of meters were analyzed throughout the Galilee. This selection leaves out most of the faults in the Galilee because they have no topographic expression (Fig. 11). This suggests that the majority of the faults in the Galilee were not active after the formation of the regional Oligocene-Miocene peneplain in the region (Garfunkel, 1988; Garfunkel and Ben-Avraham, 1996).

The escarpments that were compared with the Tur'an reference envelope are Rosh-Haniqra, Mt. Zonem, Mt. Meron, Peqi'in, Kisra, the Zurim Escarpment (including Mt. Haluz, Lavon, Tuval, Shazor, Ha'ari, Hillel, Shamai and Kefir), Gilon, Esh'har, Kamon, Livnim, Hilazon, Qoranit, Sha'abi, Hararit, Azmon, Nazerat, Tavor, Givat Hamoreh and Gilbo'a (Fig. 1). Profiles were constructed on each escarpment along lines perpendicular to the strike of the fault that formed the escarpment. Data was acquired from J. Hall's D.T.M. (Hall, 1993) at 25 meters interval using GIS technique. The altitude and distance of each profile were normalized to unity (Fig. 12) to enable the comparison of shapes of different profiles regardless of their length or height.

The faults that were analyzed were divided into three groups: one having profiles more concave than the Tur'an reference envelope, another having profiles that fall within the Tur'an reference envelope and a third one having profiles more convex than the Tur'an reference envelope. The results of the analysis are presented in Fig. 13. The comparison between the profiles indicate: (a) generally, all profiles on each

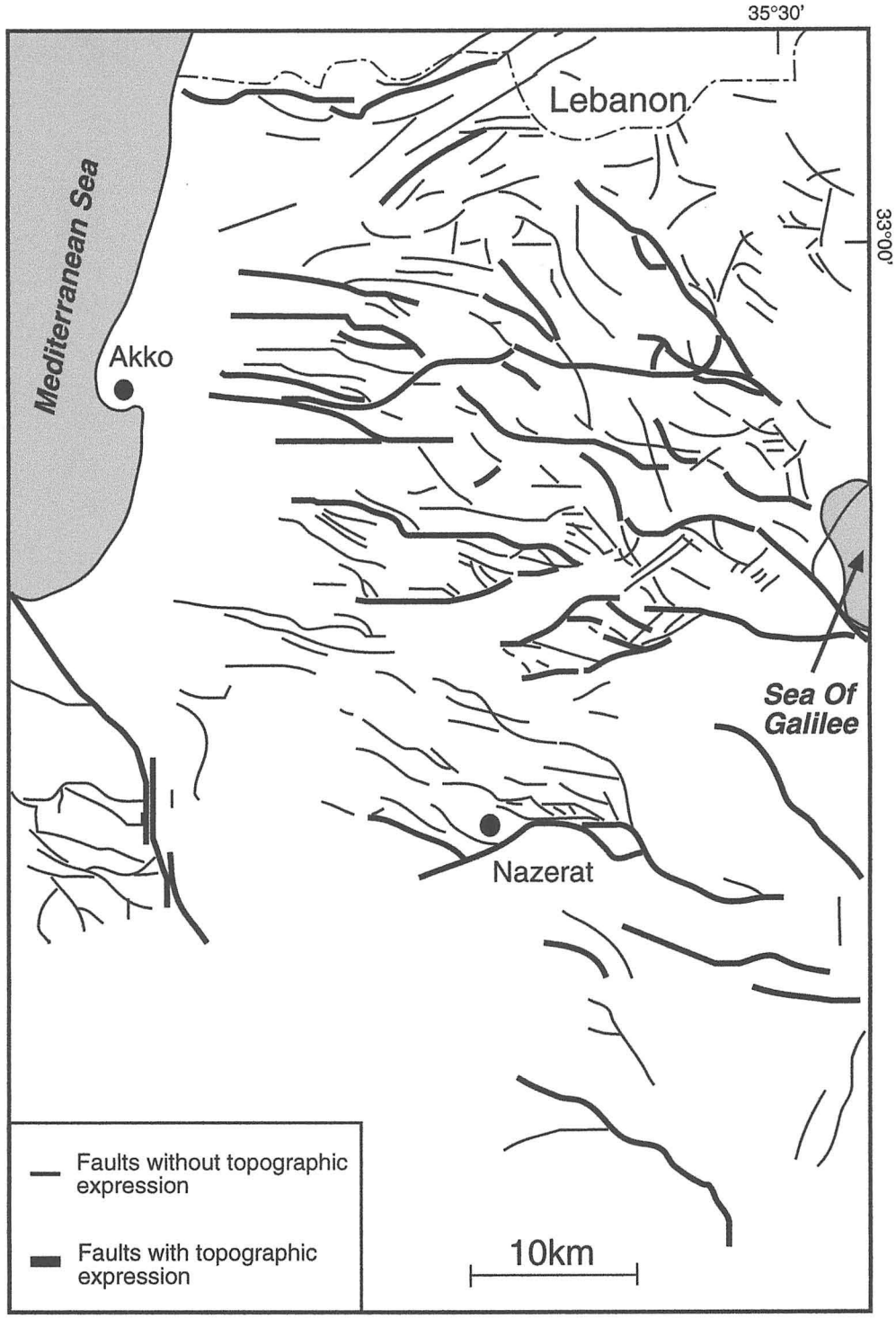


Fig. 11 – Fault map of the Galilee. The faults illustrated with a thick line have topographic expression. Most of the faults in the Galilee have no topographic expression, indicating the lack of activity after the period of denudation.

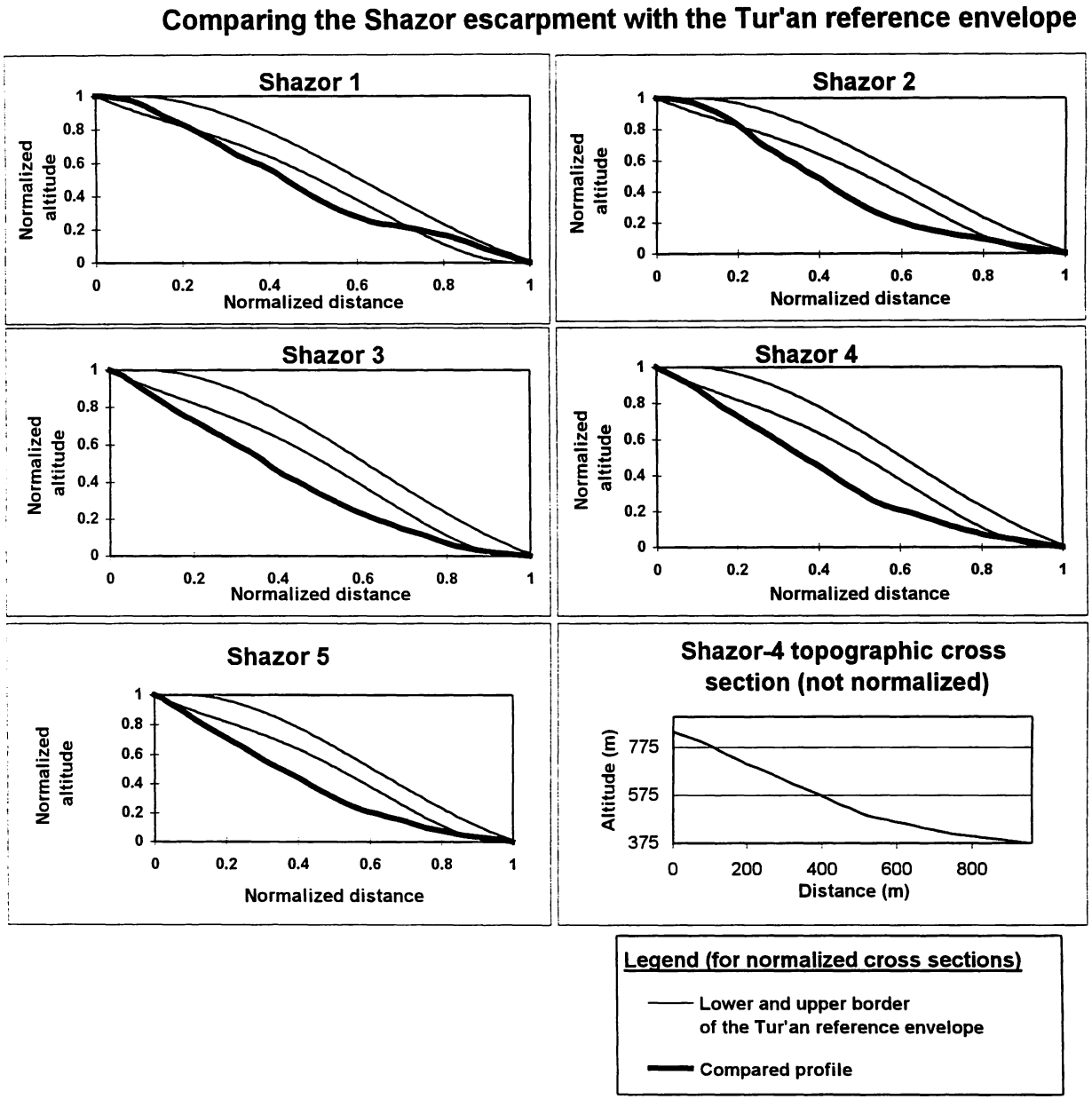


Fig. 12 –Comparison between constructed profiles along an undated escarpment (the Shazor escarpment) and the Tur'an reference envelope. The Shazor profiles are significantly more concave than the Tur'an reference envelope and therefore the Shazor escarpment is older than the Tur'an block.

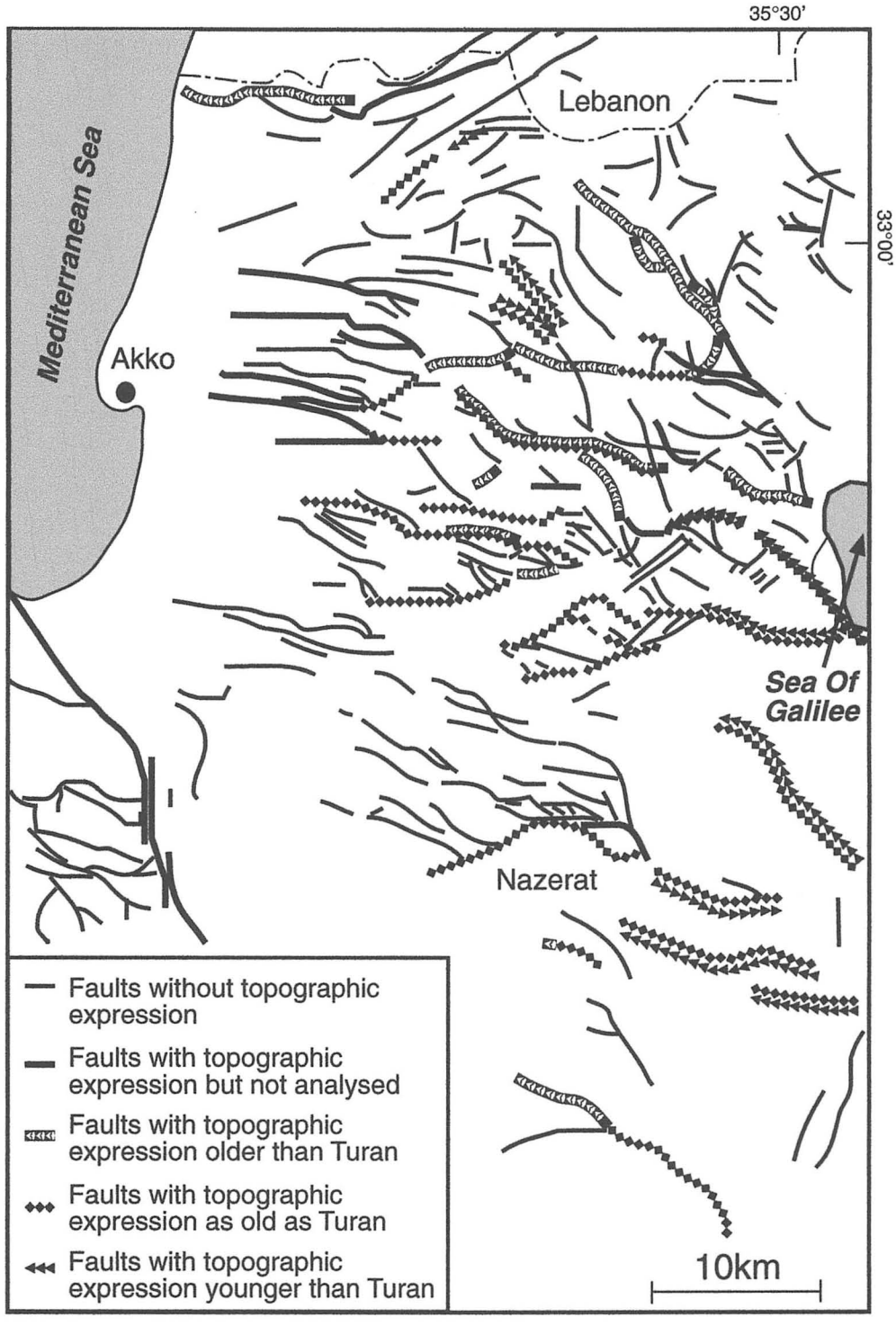


Fig. 13 – Fault map of the Galilee dividing the relief-forming faults into three age groups relative to the age of the Tur'an block. The relative age is determined by comparing the degree of concavity among the slopes of the different escarpments.

individual block-bounding fault are similar (see example Fig. 12); (b) systematic variations along fault lines occur. These variations can be correlated to segmentation deduced from L-index values (e.g. Mt. Zonem and Gilon escarpments). This indicates that different segments along a fault line experienced different long-term tectonic histories that can be expressed by variations in the slope profiles; (c) the profiles of western Mt. Zonem, Tuval, Gilon, Qoranit, Sha'abi, Azmon, Nazerat, Givat Hamoreh and eastern Gilbo'a are similar to the Tur'an reference profile and, therefore, are considered to be of similar age; (d) Mt. Haluz, Lavon and Shazor (which are part of the Zurim escarpment), Esh'har, Rosh-Haniqra, Meron, southern part of the Peqi'in fault and western Gilbo'a escarpments have concave profiles that are significantly different from the Tur'an reference envelope. This implies that these escarpments began the fast rate phase of their tectonic activity earlier than the Tur'an fault and that they were already topographic features in the Galilee four million years ago; (e) escarpments in the south-eastern part of the Galilee that are composed of an Eocene and Neogone sequence were not compared because their lithology is different than the Tur'an escarpment; nevertheless, they must be similar or younger in age to the Tur'an escarpment because they displace the Pliocene Cover Basalt; (f) many escarpments in the western Galilee have incising streams at their base; therefore it is not possible to compare them to the Tur'an escarpment; (g) escarpments that exhibit a slightly (but not significantly) more concave or convex profile than the Tur'an envelope are considered approximately of the same age as the Tur'an escarpment.

## *5.2.6 Discussion and Conclusions*

### *5.2.6.1 The Tectonic History of Mt. Tur'an*

The comparison of the different fault escarpments of the Galilee to the Tur'an escarpment is possible because the tectonic history of the Tur'an escarpment is well characterized. The difference of over 300 meters between the amount of displacement of the Turonian Bina Formation. and the 4.23 Ma Cover Basalt indicates that about half of the displacement took place prior to 4.23 Ma. Field relations in Mt. Tur'an and other outcrops of the Cover Basalt in the Galilee and the Golan indicate the basalt

spilled over a gentle landscape (Shaliv, 1991; Heimann, 1990; Heimann et al., 1996). This implies that the pre-Pliocene tectonic relief of the Tur'an fault was eroded prior to the eruption of the Cover Basalt. The question is when was that relief eroded in order to allow the Cover Basalt to flow over gentle topography?

The erosion of 300 meters of uplift prior to 4.23 Ma can be explained in two ways: (1) a long period of tectonic quiescence prevailed between the time of vertical displacement and the time of eruption of the Cover Basalt, enabling the planation of the relief formed by the tectonic activity; (2) the rate of tectonic uplift was compatible to the rate of surface erosion and topographic expression was never formed. Ron et al. (1984) show that the $\sigma 3$ direction of the regional stress field in the Galilee was East-West during the Miocene and Early Pliocene, whereas from the Middle Pliocene the $\sigma 3$ direction was vertical. This change in $\sigma 3$ direction indicates that during the earlier period of tectonic activity most of the faults were lateral with a small vertical component; thus, their topographic expression was easily eroded. However, in some cases L-index values indicate large amounts of vertical displacement during this phase. The large vertical displacement may reflect the long period that the faults were active under the East-West $\sigma 3$ direction. The later period of activity was characterized mainly by normal displacement that formed topography faster than erosion processes could obliterate it. This period of tectonic activity was shorter than the first period, and might have been accompanied by minor lateral movement.

The stress field analysis by Ron et al. (1984) supports the later explanation of compatible erosion processes and tectonic activity rates, which prevent the formation of topography. This conclusion is also supported by studying the rate of erosion of the upper surface of the Tur'an block. The permanence of the Cover Basalt over the top of the uplifted Tur'an block indicates that there has been no substantial erosion of the upper surface of the block. The minor role of erosion is also evident from the occurrence of a thick, well-developed calcretes that cover the slopes surrounding the basalt outcrop. We conclude that durinthe Plio-amount of erosion that took place on the top of the uplifted blocks was negligible; therefore, in such a time interval, morphotectonic features in the order of hundreds of meters are unaffected by erosion. The absence of erosion on the top of the uplifted block may reflect two factors: (1) the region is composed of carbonate rocks and most of the rainfall infiltrates into

underground karstic systems, so surface runoff is minimal and does not contribute to surficial erosion processes; and (2) small drainage systems exist on the uplifted blocks. Therefore, erosion of the 300 m thick uplifted section prior to the extrusion of Cover Basalt must have taken place as the tectonic relief developed. This conclusion has great significance on the understanding of the evolution of the main morphotectonic features in the Galilee. It narrows the different variations of morphotectonic development to a simple successive line of stages and simplifies the relation between uplift and truncation: an uplifted block has no topographic expression as long as the rate of truncation is comparable to uplift rate. If this quasi-equilibrium is disturbed and morphologic expression develops then the rate of erosion dramatically declines and the tectonic relief is preserved for Quaternary time scales.

The Tur'an fault system was active prior to 4.23 Ma at an uplift rate that was comparable to the erosion rate. Thus, topographic expression did not form. The Cover Basalt spilled over the gentle topography that represented this delicate equilibrium. Shortly after the Cover Basalt event, tectonic rates must have increased. Otherwise, the Cover Basalt would have been eroded as were the 300 meters of former vertical displacement. The basalt was preserved because it was lifted to an altitude high enough to avoid truncation by active streams.

It is interesting to compare the Cover Basalt on the Tur'an block with the Cover Basalt exposed near Kabul (Fig. 1) in the Lower Western Galilee. The preservation of the Cover Basalt flow on Mt. Tur'an in contrast to the preservation of only the volcanic neck in Kabul (Kafri, 1965) can be explained only by the difference in tectonic rates between these two areas. While the tectonic rate along the Mt. Tur'an fault system increased shortly after extrusion of the Cover Basalt, the rate of tectonic activity along the Kabul fault probably remained low, truncation continued, and the basalt flow was completely eroded, exposing the underlying volcanic neck.

#### *5.2.6.2 The Tectonic History of the Galilee Faults*

The tectonic history of the Tur'an block and the comparison of the Tur'an reference envelope to the other tectonic escarpments in the Galilee indicates that the normal faults in the Galilee were active during two tectonic phases: an early slow rate

phase that did not form topographic expression and a younger, higher rate phase that caused the formation of substantial topography.

Combining the L-index value calculation and the slope shape analysis for the Galilee escarpments leads to several conclusions: (1) The main escarpments in the Lower Galilee have slope profiles similar to the Tur'an escarpment, and, therefore, are of the same age, about 4 Ma. The main escarpments in the Upper Galilee (the Zurim and Meron escarpments) are more concave than the Tur'an reference envelope and seem to be older than the Tur'an escarpment. The Zurim and Meron escarpments developed earlier than those in the Lower Galilee and were morphologic features at the time the Cover Basalt flowed over the Galilee. This conclusion agrees with the existence of a thick Neogene continental sequence in the Lower Galilee and the absence of any Neogene and Pleistocene sediments in the Upper Galilee. (2) In the eastern Galilee most of the tilted blocks displace the Cover Basalt; therefore the high tectonic rate phase in this area is younger than 4 Ma. However, these escarpments cannot be compared to the Tur'an reference envelope because the stratigraphic sequence underlying the Cover Basalt consists of Neogene continental sediments and volcanic rocks (Shaliv, 1991); slope development is controlled by slope processes other than those that control the hard carbonatic slopes. Nevertheless, the persistence of the Neogene sequence implies that the eastern Galilee was a subsiding region during the Neogene (Shaliv, 1991) and a rapid uplift phase post-dated the Cover Basalt. Whether there was a slow rate phase prior to the deposition of the Neogene sequence cannot be determined by the L-index value calculation because the total normal displacement of the top of the Judea Group. cannot be obtained along the eastern Galilee fault systems. (3) The escarpments in the Galilee have a wide range of L-index values. This indicates that there is no correlation between the length of time that a fault was active at slow uplift rates and subjected to continuous truncation, and the time of increased tectonic activity and the formation of substantial topography. (4) Most of the faults in the Galilee were not active after the formation of the main erosion surface in the Galilee and are not expressed by topography. (5) Morphometric analysis of tectonic slopes in an erosional landscape is a reliable method for understanding the tectonics of a region where there is no accumulation of sediments.

## References

Achmon, M., 1986, The Carmel border fault between Yokneam and Nesher, M.Sc. Thesis, Hebrew Univ. Jerusalem, Israel (in Hebrew).

Adams, J., 1984, Large-Scale geomorphology of the Southern Alps, New Zealand, In: Morisawa, M., and Hack, J. T. (ed), Tectonic Geomorphology, Unwin Hyman.

Ahnert, F., 1966, Zur rolle der elekronische rechenmaschine und des mathematischen modells in der geomorphologie, Geogr. Z., 54, 118-133.

Ahnert, F., 1970, Functional relationships between denudation, relief, and uplift in large mid-latitude drainage basins, Amer. J. Sci., v. 268, p. 243-263.

Ahnert, F., 1973a, COSLOPE2 - a comprehensive model program for simulating slope profile development, Geocom. Bull., v. 6, p. 99-122.

Ahnert, F., 1973b, A comparison of theoretical slope models with slopes in the field, In: Schumm, S.A., and Mosley, M.P (ed), Slope Morphology, Dowden, Hutchinson and Ross, inc.

Atkinson, T.C., and Smith, D. I., 1978, The erosion of limestones, In: Ford, T.D., and Cullingford (ed), The Science of Speleology, C.H.D.

Bar, Y., and Harash, A., 1983, The analysis of young tectonic activity: the use of geomorphologic elements, Research No. 83-200-179, final report, Earth Sciences Administration, State of Israel.

Begin, Z.B., and Zilberman, E., 1997, Main stages and rates of relief development in Israel, Geol. Surv. Israel, Report GSI/24/97.

Bein, A., 1967, The hydrogeology of Cenomanian and Turonian formations in the east central Galilee, M.Sc. Thesis, Hebrew University, Jerusalem, 66p. (in Hebrew).

Bierman, P., and Turner, J., 1995, $^{10}Be$ and $^{26}Al$ evidence for exceptionally low rates of Australian bedrock erosion and the likely existence of pre-Pleistocene landscapes, Quaternary Research, v. 44, p. 378-382.

Bierman, P., Gillespie, A., Caffe, M., and Elmore, D., 1995, Estimating erosion rates and exposure ages with $^{36}Cl$ produced by neutron activation, Geochmica et Cosmochimica Acta, v. 58, no. 18, p. 3779-3798.

Bloom, A.L., 1991, Geomorphology: A systematic analysis of late Cenozoic landforms, 2nd ed., Engelwood cliffs, N.J.: Perentice-Hall, 532 pp.

Bull, W.B. 1977, Tectonic geomorphology of the Mojave Desert, U.S.G.S., Contract report 14-08-001-G-394, Office of Earth Quakes, Volcanoes and Engineering, Menlo Park, California, 188p.

Bull, W.B., and McFadden, L.D., 1977, Tectonic geomorphology north and south of the Garlock fault, California, In: D.O. Doehring (ed), Geomorphology in arid regions, Proc. Eighth Annual Geomorphology Symposium, State University of New York at Binghamton, p. 115-138.

Cohen, Z., 1988, Hydrocarbon potential of Israel, Highlights of basin analysis, O.E.I.L. Exploration Department.

Davis, W.M., 1899, The geographical cycle, J. Geogr. 14, 481.

Einsele, G., 1992, Sedimentary basins: Evolution, Facies, and Sediment Budget. Springer Verlag, Berlin, 628 pp.

Einsele,G., and Hinderer, M.,1998, Quantifying denudation and sediment-accumulation systems (open and closed lakes): basic concepts and first results, Palaeogeography, Palaeoclimatology, Palaeoecology, v. 140, p. 7-21.

Eliezri, I.Z., 1965, The geology of the Bet-Jann Region (Galilee, Israel), Isr. J. Earth Sci., v. 14, p. 51-66.

Flexer, A., Freund, R., Reiss, Z. and Buchbinder, B., 1970, Santonian Paleostructure of the Galilee. Isr. J. Earth Sci. v. 19, p. 141-146.

Freund, R., 1970, The Geometry of Faulting in Galilee. Isr. J. Earth Sci., v. 19, p. 117-140.

Garfunkel, Z., 1988, The pre-Quaternary geology of Israel, In: Yom-Tov, Y., and Tchernov, E., (ed), The zoogeography of Israel.

Garfunkel, Z., and Ben-Avraham, Z., 1996, The structure of the Dead Sea Basin. Tectonophysics, 266, 155-176.

Gerson, R., 1976, Karst and fluvial denudation of carbonate terrains under subhumid-Mediterranean and arid climates: principles, evaluation and rates (examples from Israel), In: Gams, I. (ed), Karst processes and relevant landforms, Llubljana University: 71-79.

Glikson, Y.A., 1965, Geology of the Southern Naftali mountains (north eastern Galilee, Israel), Isr. J. Earth Sci., v. 15, p. 135-154.

Golani, U., 1957, The Geology of the Meghar region. M.Sc. Thesis, Hebrew Univ. Jerusalem (in Hebrew).

Hall, J., 1993, The GSI Digital Terrain Model (DTM) project completed, Geol. Sur. Israel Curr. Res., v. 8, p. 47-50.

Hare, P.W. and Gardner, T.W. 1984, Geomorphic indicators of vertical neotectonism along converging plate margins, Nicoya Peninsula, Costa Rica, In: Morisawa, M., and Hack, J. T. (ed), Tectonic Geomorphology, Unwin Hyman.

Heimann, A., 1990, The development of the Dead Sea Transform and its margins in northern Israel during the Pliocene and Pleistocene, Geol. Surv. Israel Report GSI/28/90: 1-83. (in Hebrew, English summery)

Heimann, A., Steinitz, G., Mor, D., and Shaliv, G., 1996, The Geochronology of the Cover Basalt: Revised K-Ar and new $^{40}Ar/^{39}Ar$ results, Geol. Surv. Israel, Report GSI/6/96.

Hirano, M.A., 1968, A mathematical model of slope development – an approach to the analytical theory of erosional topography, J. Geosci. Osaka city University, 11, 13-52.

Issar, A. & Kafri, U., 1972, Neogene and Pleistocene Geology of the Western Galilee Coastal Plain. Geol. Surv. Israel, Bull. 53.

Jennings, J.N., 1971, Karst, M.I.T. press.

Kafri, U., 1963, The Geology of The Segev Region, M.Sc. Thesis, Hebrew Univ., Jerusalem (in Hebrew).

Kafri, U., 1965, The geology of the Segev area (western Galilee, Israel), Isr. J. Earth Sci, v. 14, p. 67-75.

Kafri, U., 1972, The Geological Map of Israel, 1:50000, Sheet 1-IV, Nahariyya, Geol. Surv. Israel, Ministry of Development, State of Israel.

Kafri, U., 1997, Neogene to Quaternary drainage systems and their relationship to young tectonics: Lower Galilee, Israel. Geol. Surv. Israel, Report GSI/1/97.

Kafri, U. and Ecker, A., 1964, Neogene and Quaternary Subsurface Geology and Hydrology of the Zvulun Plain. Geol. Surv. Israel, Bull. 37.

Keller, E. A., 1986, Investigation of active tectonics: use of surficial processes. In: Wallace, R.E. (ed), Active tectonics, Washington D.C. National Academy Press, p. 136-147.

King, L.C., 1957, The uniformitarian nature of hillslopes, Edin. Geol. Soc. Trans., v. 17, p. 81-104.

Levy, Y., 1983, The Geological Map of Israel, 1:50000, Sheet 3-II, Shefar'am, Geol. Surv. Israel, Ministry of Development, State of Israel.

Matmon, A., Enzel, Y., Zilberman, E., and Heimann, A., (in press), Late Pliocene and Pleistocene reversal of drainage systems in northern Israel: tectonic implications, Geomorphology.

Mayer, L., 1986, Tectonic Geomorphology of Escarpments and Mountain Fronts, In: Wallace, R.E. (ed), Active tectonics, Washington D.C. National Academy Press, 125-135.

Menges, C.M., 1988, The tectonic geomorphology of mountain front landforms in the Northern Rio-Grande Rift near Taos, New Mexico, Ph.D. Dissertation, The University of New Mexico, Albuquerque, New Mexico.

Michelson, H., 1970, Geological map of Western and Central Galilee, compilation map, TAHAL, Tel-Aviv.

Nir, D., 1970, Geomorphology of Israel, Aqademon, 404 pp.

Ollier, C.C., 1981, Tectonics and Landforms, Longmans, New York, 324pp.

Picard, L., 1943, Structure and evolution of Palestine with comparative notes on neighboring countries, Hebrew Univ. Jerusalem, Geol. Dept., Bull. 4, 134 pp.

Picard, L., and Golani, U., 1965, The Geological Map of Israel, 1;250000, Northern Sheet,

Retallack, G.J., 1990, Soils of the past, Unwin Hyman, Boston, 520 pp.

Ritter, D.F., Kochel, R.C., and Miller, J.R., 1995, Process Geomorphology, 3rd ed., WCB.

Rockwell, T.K., Keller, E.A., and Dembroff, G.R., 1988, Quaternary rate of folding of the Ventura Avenue Anticline, western Transverse Ranges, Southern California, Geol. Soc. Amer. Bull. 100, 850-858.

Ron, H., Freund, R., Garfunkel, Z., and Nur, A., 1984, Block rotation by strike slip faulting: structural and paleomagnetic evidence. J. Geophys. Res., 89, 6256-6270.

Saltzman, U., 1964, The geology of the Tabha-Huquq-Migdal area, M.Sc. Thesis, Hebrew Univ. Jerusalem (in Hebrew).

Schulman, N., 1962, The geology of the Central Jordan valley, Ph.D. Thesis, The Hebrew University, Jerusalem (in hebrew).

Shaliv, G., 1991, Stages in the tectonic and volcanic history of the Neogene Basin in the Lower Galilee and the valleys, Geol. Surv. Israel, Repor/11/91.

Shlein, N., 1961, The Geology of the Alma region. M.Sc. Thesis, Hebrew Univ. Jerusalem (in Hebrew).

Simons, M., 1962, The morphological analysis of landforms: a new review of the work of Walter Penck (1888-1923), Trans. Inst. Br. Geol., 31, 1-14.

Sivan, D., 1996, Paleogeography of the Galilee Coastal plain During the Quaternary, Geol. Surv. Israel, Report GSI/18/96 (in Hebrew).

Sparling, D.R., 1967, Anomalous drainage pattern and crustal tilting in Ottawa County, Ohio, Ohio J. Sci. 67, 378-381.

Strahler, A. H., and Strahler, A. N., 1992, Modern physical Geography, 4th ed., John Wiley & Sons, Inc.

Trudgill, S., 1985, Limestone Geomorphology, Longman.

Twidale, C.R., 1971, Structural Landforms, Australian National University Press, Canberra.

Vroman, A., 1958, The geological map of Israel, 1:50000, Series 1, Galilee, Sheet 1, Geol. Surv. Israel.

Wells, S.G., Bullard, T.F., Menges, C.M., Drake, P.G., Karas, P.A., Kelson, K.I., Ritter, J.B., and Wesling, J.R., 1988, Regional Variations in Tectonic Geomorphology Along a Segmented Convergent Plate Boundary, Pacific Coast of Costa Rica, Geomorphology, 1, 239-265.

Yair, A., 1962, The morphology of Nahal Dishon, M.Sc. Thesis, Hebrew Univ. Jerusalem, Israel (in Hebrew).

# PUBLICATION DOCUMENTATION PAGE

| | | |
|---|---|---|
| 1. Publication No<br>Es-38-98. | 2. | 3. Recipiont Accession No. |
| Title and Subtitle: **Morphometric analysis for determining the age of escarpments: an example from the Galilee, northern Israel** | | 5. Publication Date: 2/99 |
| Author(s): A. Matmon, E. Zilberman, anf Y. Enzel | | 6. Performing Organiz. Code: |
| 9. Performing Organization Name and Address<br>המכון הגיאולוגי<br>מלכי ישראל 30, ירושלים 95501 | | 10. Project/Task/Work Unit No.<br>11. Contract No. |
| 12. Sponsoring Organization(s) Name and Address<br>(a) Ministry of National Infrastructures<br>Earth Science Administration<br>(b) המכון הגיאולוגי, משרד האנרגיה והתשתית | | 13. Type of Report and Period Covered:<br>---<br>14. Sponsoring Organiz. Code |
| 15. Supplementary Note | | |


Abstract .16

Dating of tectonic activity in erosional landscapes is problematic because dateable sediments are absent. We use GIS-based morphometric analyses of escarpments bounded by normal faults in the Galilee as a tool to determine their relative ages. Two morphometric parameters are used to discriminate tectonic phases in this extensional region: a) The ratio L between the height of the escarpment and the total stratigraphic displacement, b) The shape of the topographic profile of each escarpment relative to a slope profile of known age (Mt. Tur'an). Systematic changes in L-index values along a fault are indicative of segmentation. By comparing the profile shapes it is possible to determine the relative timing for a change in rates of displacement from slow, continuous and landscape-truncating phase, to a fast topography-forming phase. The reference slope of Mt. Tur'an, is ~300 meters high and was formed by the Tur'an fault system, which has a total displacement of 625 m. A basalt flow dated at 4.23±0.23 Ma is displaced 300 m, which is identical to the topographic expression of this escarpment. The L-index value for this escarpment is ~0.5. Accordingly, the Tur'an fault system was active prior to 4.23 Ma at slow uplift rates that enabled truncation to maintain the gentle slope over which the basalt flowed. Increased tectonic rates following the basalt extrusion led to the formation of the escarpment. The preservation of the basalt at the top of the escarpment indicates that erosional lowering of the upper surface of the Tur'an block has been no minor since its formation. Comparisons between the Tur'an reference profile and other escarpments were used to establish the relative ages of activity on their bounding faults. We conclude that (a) the topographic profiles of different parts of each individual escarpment have similar shapes; (b) there are systematic variations in profiles along escarpments that fit the segmentation deduced from the L-index values; (c) escarpments more concave or convex than the reference escarpment are older or younger than 4 Ma, respectively, and (d) The Galilee escarpments did not form simultaneously. A few were already major morphotectonic features by the Early to Middle Pliocene and the rest are younger, having formed between 4-2 Ma.


| | | |
|---|---|---|
| 17. Identifiers/Key Words/Descriptors: Galilee, Escarpments, Tectonics, Slope erosion | | |
| 18. Availability Statement<br>unpublished | 19. Security Class<br>(This Report)<br>--- | 21. No. of Pages: 35<br>--- |